UNIVERSITY OF CALIFORNIA
RIVERSIDE

Fluorescence Biosensing of Therapeutic Drug Concentrations in Biological Fluids

A Dissertation submitted in partial satisfaction
of the requirements for the degree of

Doctor of Philosophy

in

Bioengineering

by

Jacob Matthew Vasquez

December 2016

Dissertation Committee:
Dr. Valentine I. Vullev, Chairperson
Dr. Kaustabh Ghosh
Dr. William H. Grover

The Dissertation of Jacob Matthew Vasquez is approved:

_____

_____

_____

Committee Chairperson

University of California, Riverside

ACKNOWLEDGMENTS

I am incredibly grateful to my professor, Dr. Valentine Vullev, for taking me as a graduate student and investing his time and effort into developing me as a scientist. His dedication to his students, seemingly unending knowledge and devotion to science has been a constant source of motivation and inspiration. His belief in me and my abilities has helped me to pursue my dreams and has left me forever grateful. Thank you for being the mentor that every graduate student should have.

I am thankful to my committee members: Dr. Kaustabh Ghosh & Dr. William Grover for their support and helpful advice. I would like to sincerely thank the faculty and staff of the Department of Bioengineering for providing me with support throughout the years.

I would like to thank the National Science Foundation and University of California, Riverside for supporting my graduate studies with the Louis Stokes Alliances for Minority Participation, Bridge to the Doctorate Fellowship (NSF –LSAMP). I would also like to thank Dr. Natasha Raikhel and Dr. Craig V. Byus for giving me my first opportunities in a research environment.

I would sincerely like to thank my fellow Vullev Group members (Past and Present). To Dr. Marlon Thomas, Sean Guthrie M.S., Andrew Vu, Dr. Elizabeth Zielins, Dr. Duoduo Bao, Ali Hadian M.S., Dr. Srigokul Upadhyayula, Dr. Sharad Gupta, Dr. Vicente Nunez, Eli Espinosa (PhDc), Max Mayther (PhDc) and Dr. Jillian Larsen-Clinton, your support, encouragement and most importantly your friendship is something that I will remember with fondness for the rest of my life.

I am grateful to have worked with the talented undergraduates; Areio Hashemi, Cheyann Wettland, Novanjott Batth, Sunghoon Bae, Beomjoon Kim and Sephr Halabian.

Thank you Vullev Lab family, for all your love and friendships and thank you to my academic grandfather Prof. Guilford Jones, II, for his legacy.

I want to thank the Journal of Biotechnology Progress for publishing the research in Chapter 2.

DEDICATION OF THE DISSERTATION

I dedicate this dissertation to my patient, loving family. Your support, encouragement and love is what drives me forward.

My Beloved Wife: Dr. Casandra J. Vasquez (UCR Entomology)
My Beautiful Children: Miss Laurelei J. and Mr. Simon J. Vasquez
My Mother: Ms. Deborah Corona-Vasquez
My Father: Mr. Matthew S. Vasquez
My Sisters: Aileen Vasquez-Cortez; Rebecca Vasquez-Solorio and Johanna Garcia
In Honor of My Grandparents:
Joe and Tencia Vasquez
David Corona and Lupe Medina
I love you all!

ABSTRACT OF THE DISSERTATION

Fluorescence Biosensing of Therapeutic Drug Concentrations in Biological Fluids

by

Jacob Matthew Vasquez

Doctor of Philosophy, Graduate Program in Bioengineering
University of California, Riverside, December 2016
Dr. Valentine I. Vullev, Chairperson

Our work focuses on routes toward fluorometric methodologies for detecting warfarin, an anticoagulant used in the management of a variety of thromboembolic disorders. Warfarin (a.k.a. Marevan, Coumadin, Waran, Jantoven) is one of the most widely prescribed medications for preventing thromboembolic events (blood clots). It is a drug with a narrow therapeutic index placing a strict requirement for careful monitoring of the patients taking it. In order to ensure that the effective physiological result is achieved and maintained, the dose must be adjusted accurately and frequently. Currently, estimation of the international normalized ratio (INR) of the prothrombin time (PT) is the most common method used for monitoring warfarin therapy. This estimation is actually a measure of the physiological result of a dose taken up to 72 hours prior. A rapid and clinically deployable method for measuring warfarin in blood plasma in real-time are needed in combination with PT/INR to further predict concentrations and prevent lapses in patient compliance, such as changes in diet and interactions with other medications that

can result in falling out of the warfarin therapeutic range. Due to their inherently high sensitivity, fluorescence techniques are a preferred approach for the development of biosensing applications. Warfarin, a derivative of coumarin, absorbs and fluoresces in the UV region of the spectrum. Hence, it is immensely challenging and impractical to use warfarin fluorescence for its detection in biological fluids due to the presence of other UV-absorbing chromophores and fluorophores. The utilization of warfarin's inherent properties and structural dependence on media pH, provides a direct handle for warfarin sensing. Herein, we characterized the photophysical properties of warfarin in solvents with varying temperature, polarity and viscosity, while also demonstrating rapid extraction and quantification of warfarin from aqueous and blood plasma samples using fluorescence spectroscopy.

Table of Contents

Chapter 3

Microextraction of warfarin from blood plasma using differential fluorescence analysis

List of Schemes

List of Tables

List of Figures

Chapter1. Introduction

Chapter2. Fluorescence Enhancement for Warfarin Sensing

Figure 3-2, p75
Concentration dependence of absorbance and fluorescence of warfarin for 1-octanol in the presence of 8% v/v hexylamine and 25mM deproteinating agent trichloroacetic acid (λ_{ex} = 310 nm). (a) Fluorescence spectra for different concentrations of warfarin (2 – 100 □M). (b) Dependence of integrated emission intensity on warfarin concentration The non-linear fit is based on eq. 1.
[NEED TO CORRECT THE TEXT FOR THIS GRAPH]

Figure 3-3, p76
Acidic vs. Basic sample extraction of warfarin into 1-octanol. Absorption spectra of 25 μM warfarin extracted into 1-octanol, from acidic (solid), and basic (dashed) aqueous solutions. (10 μL hexylamine was added to 0.120 ml of recovered Octanol; hexylamine 8% v/v final). Warfarin was dissolved into phosphate buffered solutions (25 □M). Warfarin/PBS solutions (1.25 mL), was either diluted with water (basic) or 10% trichloroacetic acid (acidic) per extraction protocol.

Figure 3-4, p77
Concentration dependence of the extraction efficiency of warfarin from aqueous solutions of BSA. Mean extraction efficiency of warfarin dissolved in protein media (2.0-100 $X10^{-6}$ M). Integrated fluorescence intensity of warfarin extracted from basic protein media into 1-octanol. (λ_{ex}=310nm).

Figure 3-5, p78
Interpolation of aqueous dose from fluorescence

Figure 3-6, p79
Concentration dependence of fluorescence of warfarin for 1-octanol (λ_{ex} = 310 nm). (a) Dependence of integrated emission intensity spectra for different concentrations of warfarin (2 – 24 □M) in 1-octanol (open circle). (b) Dependence of integrated emission intensity on warfarin extracted from blood plasma (solid). The non-linear fit is based on eq. 1.

Figure 3-7, p80
Concentration dependence of fluorescence of warfarin for 1-octanol (λ_{ex} = 310 nm). (a) Dependence of integrated emission intensity spectra for different concentrations of warfarin (2 – 100 □M) in 1-octanol (open circle). (b) Dependence of integrated emission intensity on warfarin extracted from blood plasma (solid). The non-linear fit is based on eq. 1.

Figure 3-8, p80
Dependence of absorbance and fluorescence of 7-methoxycoumarin (7MC) for acidic and basic conditions (λ_{ex} = 310 nm). (a) Absorption and fluorescence spectra of 5 □M 7MC dissolved in 1-octanol. (b) Absorbance and emission spectra of octanol extracted from blood plasma (4 μM warfarin + 5 □M 7MC). (c) Concentration comparison of warfarin extracted from plasma with and without contaminants.

Chapter 1

Introduction

CHAPTER 1:

1.1 Introduction

1.1.1 Identification and Historic Perspective of Coumarin Based Anticoagulants

The most widely prescribed anticoagulant in the world, warfarin, can be found in the daily medication regiments of a large percentage of persons over 80 years old.[1,2] The emergence of warfarin as a drug of therapeutic potential can be traced back to incidences of healthy cattle across the prairies and plains of Canada and North America dying of internal bleeding for no apparent reason. During this time, the great depression was stifling economic prosperity across the United States, and losses of this commodity, livestock, directly affected the livelihood of the cattle farmers involved. The absence of an easily identifiable cause for this hemorrhagic disease, forced every viable factor to be explored.

The livestock affected in both Canada and the United States had grazed on European varieties of hay, white *Melilotus alba* and yellow *Melilotus officinalis* sweet clover hay.[3] It was noted that the frequency of hemorrhagic incidences increased with wet climate conditions. Wet conditions invariably enhanced the proliferation of molds such as those identified as infecting stored sweet clover hay, *Penicillin nigricans* and *Penicillin jensi*. The mold infected hay was later identified as being a crucial and corollary to the hemorrhagic disease affecting the livestock.[4] The use of moldy hay was not a normal practice, but due to the economic climate of late 1920s agriculture, feed waste was a luxury few cattle farmers could afford.

The early work of two veterinarian surgeons, Canadian F.W. Schofield, and American L.M. Roderick, provided crucial insights into the cause and defect of sweet clover disease, namely, showing the direct link between livestock deaths and moldy sweet clover[3], followed by the observation that the disease was biphasic. The temporal trajectory of this hemorrhagic "sweet clover" disease manifests as an elongation of the prothrombin time within 15 days' post-ingestion, with terminal manifestation, spontaneous hemorrhage, occurring within 30 to 50 days.[4] Discovery that the clotting factor prothrombin suffered from reduced activity, Roderick was able to show that the disease was reversible, when an affected animal was transfused with fresh blood.

These insights by Schofield and Roderick offered the first tangible protocols to address the hemorrhagic disease. It took the help of a Wisconsin farmer, Ed Carlson, who after losing much livestock to sweet clover disease, transported a dead cow, and a large volume of unclotted blood to the lab of Karl P. Link at the University of Wisconsin. Although the cause of the hemorrhagic disease had been shown, the active compound, which up to this point had yet to be identified and isolated. Link began work on this problem in 1933, with a initial focus aimed at the development of an in-vitro clotting assay using plasma from rabbits to guide subsequent chemical fractionation of compounds isolated from molded/affected hay. Following several years of work by Links laboratory group, the compound was subsequently crystallized.[3] The identification of this isolate was determined to be that of dicoumarol, 3,3'-methylene-bis(4-hydroxycoumarin). Link had discovered that the rotting sweet clover contained a compound, coumarin. Further investigation revealed that the coumarin originated not from the clover itself, but as a side

effect of mold mediated metabolic conversion of hay material to coumarin. The mechanism by which dicoumarol is synthesized, starts with coumarin oxidation to 4-hydroxycoumarin, followed by a subsequent formaldehyde facilitated coupling step to another coumarin moiety to form dicoumarol.[3] Dicoumarol was patented in 1941. The work was funded by the Wisconsin Alumni Research Foundation (WARF), and patent rights for dicoumarol were given to WARF in 1941 by Link. In the 1950s, dicoumarol was replaced by a smaller synthetic analogue, Coumadin, named also Warfarin. Incidentally, warfarin was first commercialized in 1948 as a pesticide.

1.1.2 Warfarin Indications/Monitoring

The Food and Drug Administration (FDA) estimates that warfarin is prescribed to approximately 2 million new patients annually to prevent myocardial infarctions and hemorrhagic or ischemic stroke (Figure 1). The clinical significance of warfarin lies in its ability to act as a potent anticoagulant. The synthetic pathway of hepatic vitamin-K dependent clotting factors (II, VII, IX, X) and hepatic proteins (C, S) is interrupted by warfarin-induced inhibition of vitamin K_1 epoxide regeneration, resulting in anticoagulance.[5] Complications arising from warfarin therapy are categorized into two subgroups, hemorrhagic and non-hemorrhagic side effects, which include internal bleeding and skin necrosis, respectively.[6,7] Warfarin is a medication with a narrow therapeutic index (NTI) that requires close monitoring to prevent thromboembolic complications attributed to over- and under- anticoagulation. Optimal dosage of warfarin, however, varies among

individuals due to factors such as age, genetics, diet and medications taken concurrently.[8] According to the FDA, warfarin is the **second largest cause** of emergency-room visits due to drug complications, after insulin.[6]

Currently, the daily dose of warfarin and its clotting activity in individual patients is empirically estimated using a prothrombin-time (PT) test, which measures how long it takes for the blood to clot via the extrinsic coagulation pathway. Patients' PT results are compared with the PT values for healthy individuals and normalized with an international sensitivity index (ISI) to yield an international normalized ratio (INR), which provide the guidelines for warfarin dosage.[1] ISI is another empirical parameter introduced for accounting for the differences in the potencies of the various thromboplastin extracts used for the PT tests.[9] This pharmacodynamics analytical approach, however, does not necessarily produce results that allow for facile regulation of the warfarin daily dose.[10] It can take 24 hours for the PT values to reflect the changes in the warfarin dosage. Furthermore, PT values cannot distinguish between crucial factors such as change in the patients' diet, interference with other medication, and changes in the metabolic dynamics of processing the warfarin out of the body. This uncertainty in the factors that influence the PT values results in PT fluctuations and challenges with stabilizing the patients' warfarin dosage. Such PT instability is especially pronounced in pediatric patients, whose suppressed fibrinolytic system and variable levels of coagulation factors, such as vitamin K, protein C, protein S, antithrombin and a2-macroglobulin, complicate anticoagulant management.

The possible complications, coupled with the annual increase of new patients with prescribed warfarin therapeutics, warrants the development of assays facilitating fast, accurate and quantitative direct monitoring of NTI medications, such as warfarin. In recent years, there has been increasing interest in developing methods for measuring the concentration of warfarin in blood plasma (ranging up to about 16 μM) in order to establish improved protocols aimed for personalization of the needs of each individual.[19,26,10,1127] Current analytical methods for establishing the free-warfarin plasma concentration[12,13] have complexity that prevents them from being carried out in a clinician's office or by a patient at home. Furthermore, the clearance of warfarin from the blood is somewhat complex and does not follow simple first order pharmacokinetics.[10]

This research has the potential to lead to a warfarin test methodologies based on a native target protein that has the potential to become a point-of-care (POC) technology. The methodology will have an impact not only on the clinical diagnosis and medication dosing, but also on biomedical research. Using the envisioned warfarin sensor by clinicians and patients, in parallel with coagulometeric tests, will provide valuable insight about correlations between the blood coagulance and the blood concentration of warfarin.

1.1.3 Our approach

The initial concept involved macromolecular fluorescence sensors, utilizing photo-induced electron transfer (PET), comprised two principal components: (1) auxiliary

fluorophores (Figure 2); and binding site template for warfarin. For templates carrying warfarin binding sites, β-cyclodextrin and helix bundles of synthetic polypeptides with amino acid sequences based on vitamin K epoxide reductase (VKOR), an enzyme for which warfarin is an inhibitor were experimentally and computationally explored.

To address the first component, auxiliary fluorophores, different photoprobes were utilized that fluoresce at different wavelengths spread throughout the visible region of the spectrum: i.e., the excitation energies, E_{00}, range between about 1.7 and 3.0 eV. The fluorescence of these photoprobes should be quenched to a different extent by warfarin: i.e., the emission of some of the photoprobes should be completely quenched, some partially quenched, and some not quenched at all by warfarin.

Using cyclic voltammetry, I dermined the redox properties of warfarin was determined. For aprotic solvent media (i.e., acetonitrile), warfarin undergoes irreversible oxidation resulting an anodic peak at about 1.1 to 1.2 V vs. SCE (for different scan rates) and no cathodic peak. The positions of the anodic peaks for the various scan rates imply that the warfarin oxidation potential is about 1.1 V vs. SCE. Thus, warfarin is a moderately good electron donor. UV absorption and emission spectra revealed that the excitation energy of warfarin, E_{00}, is about 3.6 eV, indicating that its reduction potential is about –2.4 V vs. SCE. Therefore, warfarin cannot act as an electron acceptor for the proposed sensor. Our findings from electrochemical and spectroscopic measurements supported the proposed sensor designs, in which warfarin would act as an electron donor.

Using Stern-Volmer analysis, I tested the extent to which warfarin quenches the fluorescence of potential photoprobes with different excitation energies (i.e., color of

fluorescence) and oxidation potentials: 10-methyl-N-phenylacridinium (Ph-Acr), N-phenyl-dimethylaminonaphthalimide (Ph-ANI) and sulforhodamine B (SRh-B). The oxidation potentials of Ph-Acr, Ph-ANI and SRh-B are –0.55, –1.4 and –0.56 V vs. SCE, respectively, with fluorescence maxima at 505 nm, 525 nm and 585 nm, respectively. As expected from the predicted charge-transfer kinetics, the Stern-Volmer analysis yielded different bimolecular quenching constants for the three different fluorophores: 4×10^{9}, 8×10^{7} and 4×10^{8} M^{-1} s^{-1} for Ph-Acr, Ph-ANI and SRh-B, respectively. The diffusion-limited value of the bimolecular quenching constant for PhAcr indicates that the acridinium conjugate and warfarin undergo efficient PET. The PET between warfarin and the other two photoprobes was not as efficient because, in comparison with Ph-Acr, Ph-ANI has significantly more negative reduction potential and SRh-B has smaller excitation activation energy. This difference in the warfarin-induced quenching efficiency of differently colored fluorophores demonstrated the principle of generating "fluorescence fingerprints" for warfarin in the visible region of the spectrum.

To address the second component of the initial concept, the florescence properties of warfarin allowed me to monitor its binding to cyclodextrins (Chapter 2). Upon binding to cyclodextrin, the emission quantum yield of warfarin increased three- to four-fold. I demonstrated that the increase in the fluorescence quantum yield resulted from restrictions of the molecular motions of warfarin, induced by the binding site, and not from the lower polarity of the binding microenvironment.[14] This quantum yield increase provides distinction between bound and free warfarin. We also developed a two-dimensional linear model that allows for obtaining the binding constant and the binding stoichiometry from

fluorescence titration data. I determined that warfarin binds to β-cyclodextrin at 1:1 stoichiometry, with a binding constant of about 300 M^{-1}. Because of the relatively small binding constant, we shifted our focus onto VKORC1 protein systems that have a strong affinity for warfarin.

Vitamins K, a group of lipophilic derivatives of 1,4-naphthaquinone, [5] play a crucial role in the coagulation of blood. Via γ-glutamyl carboxylase, 1,4-hydronaphthaquinones (i.e., reduced derivatives of vitamin K) facilitate the post-translational carboxylation of glutamates in coagulation factors II, VII, IX and X, and proteins S, C, and Z. (γ-glutamates comprise calcium binding sites essential for the coagulation-chain processes.) The enzymatic glutamate carboxylation yields vitamin K 2,3-epoxide derivatives. A multiprotein complex, vitamin K epoxide reductase (VKOR), recycles the formed epoxides back to the corresponding vitamin K hydroquinones. Vitamin K epoxide reductase complex subunit 1 (VKORC1) is a transmembrane enzyme, which has a strong binding affinity for coumarin derivatives, such as warfarin. Upon binding, warfarin inhibits VKORC1, i.e., warfarin is a vitamin K antagonist. Human VKORC1 can be readily expressed and its sequence is known.[8] Point-mutation studies have revealed the residues crucial for warfarin binding affinity of this transmembrane protein.[8] The tertiary structure of the human VKORC1, however, is not known. The recently reported crystal structure of the bacterial VKOR analogue (*Synechococcus* sp.)[15] will allow for revealing structural features of the human VKORC1 via homology studies. I complied a structural model of the human VKORC1 from its amino acid sequence and from the three-dimensional crystal structure of a related "homologous" template protein, the bacterial VKOR. The thus

generated alignment map was used for producing a structural model of the target protein, VKORC1.

I used the homology-modeling package MODELLER (UCSF) for homology/ comparative modeling of protein three-dimensional structures.[16] Molecular-modeling studies for structural predictions employ preexisting three-dimensional structure of a protein homologue template. In this case, the template was bacterial Vitamin K epoxide reductase (VKOR, PDB 3KP9). This template allowed me to model the predominant form of the targeted protein, Vitamin K epoxide reductase complex subunit 1 (VKORC1_HUMAN, UniProtKB/Swiss-Prot Q9BQB6). A sequence alignment of the bacterial VKOR template and human VKORC1 allowed me to calculate a homology model containing all heavy atoms. MODELLER implemented comparative protein structure modeling by satisfaction of spatial restraints. Due to relatively small sequence homology, 24%, between the human and bacterial analogues, and sequence variability around the warfarin binding pocket, alternative methods utilizing colorimetric and direct fluorescence detection of warfarin were needed.

Access to, and extraction of drugs which are highly bound by plasma proteins is a challenge for direct colorimetric and fluorescence detection in biological fluids (warfarin is greater than 99% protein bound).[17] Several methods were utilized to enable warfarin detection and quantification in biological fluids. The first two methods involved directly targeting the methyl ketone moiety of warfarin to provide a colorimetric handle, while the third method sought to directly extract and quantify warfarin from blood plasma.

Haloform reaction. A microanalytical method for the determination warfarin in human blood serum, the haloform reaction proceeds under mildly alkaline conditions, to warfarin affords stoichiometric proportions of haloform and 3-(4-Hydroxy-2-oxo-2H-chromen-3-yl)-3-phenylpropanoic acid. The haloform generated served as a direct measure (via Fujiwara reaction) of methylkentone containing species such as warfarin.

Fujiwara reaction**.** Liberated haloform from the Haloform reaction was converted to the Fujiwara-type chromophores (λ_{max} = 360 nm, Glutaconaldehyde; λ_{max} = 421 nm, *N-[(1E,3E)-4-methanoyl-1,3-butdienyl]*benzenecarboxamide, and λ_{max} = 536 nm [N^2-[(1*E*,3*E*)-1,3-butadienyl]-N^1-(1,3-butadienyl)benzamidine) with a pyridine-water-sodium-hydroxide mixture.[18] The method responds to nanomolar concentrations of warfarin. I investigated the feasibility of warfarin detection via the Haloform and Fujiwara reactions at physiological concentrations. Serum samples with warfarin were treated with Sodium dichloroisocyanurate dehydrate to generate stoichiometric proportions of chloroform.

1.1.4 Direct measurement & quantification of warfarin concentration in plasma.

Microextraction,[19] coupled with absorbance and fluorescence spectroscopic analysis, provides a means for a relatively simple method for quantification of warfarin in blood samples. We utilize the inherent pH-dependent tautomerization of warfarin for optimization of its extraction efficiency and spectroscopic quantification.[20,21] This pH dependence proves especially important for utilizing differential emission for eliminating

the adverse effect from fluorescent contaminants. This method offers working range across the physiologically relevant concentrations, while utilizing relatively small volumes of biological sample (Chapter 3).

In summary, the most important contributions from my doctoral work are: (1) the identification of warfarin-induced quenching efficiency of differently colored fluorophores "fluorescence fingerprints" for warfarin in the visible region of the spectrum; (2) the determination that warfarin binds to β-cyclodextrin at 1:1 stoichiometry; and (3) a microextraction method utilizing absorbance and fluorescence spectroscopic analysis for the determination of warfarin in blood plasma.

1.2 References

(1) Guyatt, G. H.; Norris, S. L.; Schulman, S.; Hirsh, J.; Eckman, M. H.; Akl, E. A.; Crowther, M.; Vandvik, P. O.; Eikelboom, J. W.; McDonagh, M. S.; Lewis, S. Z.; Gutterman, D. D.; Cook, D. J.; Schünemann, H. J. *Chest* **2012**, *141* (2), 53S – 70S.

(2) Juurlink, D. N. *Can. Med. Assoc. J.* **2007**, *177* (4), 369–371.

(3) Link, K. P. *Circulation* **1959**, *19* (1), 97–107.

(4) Francis, C. W. *Hematology* **2008**, *2008* (1), 251–251.

(5) Danziger, J. *Clin. J. Am. Soc. Nephrol.* **2008**, *3* (5), 1504–1510.

(6) Hamby, L.; Weeks, W. B.; Malikowski, C. *Eff. Clin. Pract. ECP* **2000**, *3* (4), 179–184.

(7) Sahu, K. K.; Varma, S. C. *Indian J. Med. Res.* **2016**, *143* (4), 528–529.

(8) Jorgensen, A. L.; Al-Zubiedi, S.; Zhang, J. E.; Keniry, A.; Hanson, A.; Hughes, D. A.; Eker, D. van; Stevens, L.; Hawkins, K.; Toh, C. H.; Kamali, F.; Daly, A. K.; Fitzmaurice, D.; Coffey, A.; Williamson, P. R.; Park, B. K.; Deloukas, P.; Pirmohamed, M. *Pharmacogenet. Genomics* **2009**, *19* (10), 800–812.

(9) Gosselin, R.; Owings, J. T.; White, R. H.; Hutchinson, R.; Branch, J.; Mahackian, K.; Johnston, M.; Larkin, E. C. *Thromb. Haemost.* **2000**, *83* (5), 698–703.

(10) Breckenridge, A.; Orme, M. *Clin. Pharmacol. Ther.* **1973**, *14* (6), 955–961.

(11) Midha, K. K.; McGilveray, I. J.; Cooper, J. K. *J. Pharm. Sci.* **1974**, *63* (11), 1725–1729.

(12) Qayyum, A.; Najmi, M. H.; Khan, A. M.; Abbas, M.; Naveed, A. K.; Jameel, A. *Pak. J. Pharm. Sci.* **2015**, *28* (4), 1315–1321.

(13) Shen, Y.; Xiang, J.; Liang, M.; Yu, Q.; Nan, F.; Qin, Y. *Sichuan Da Xue Xue Bao Yi Xue Ban* **2016**, *47* (1), 106–110.

(14) Wan, J.; Ferreira, A.; Xia, W.; Chow, C. H.; Takechi, K.; Kamat, P. V.; Jones, G.; Vullev, V. I. *J. Photochem. Photobiol. Chem.* **2008**, *197* (2-3), 364–374.

(15) Tie, J.-K.; Stafford, D. W. *Vitam. Horm.* **2008**, *78*, 103–130.

(16) Yang, Z.; Lasker, K.; Schneidman-Duhovny, D.; Webb, B.; Huang, C. C.; Pettersen, E. F.; Goddard, T. D.; Meng, E. C.; Sali, A.; Ferrin, T. E. *J. Struct. Biol.* **2012**, *179* (3), 269–278.

(17) Sastry, C. S.; Rao, T. T.; Sailaja, A.; Rao, J. V. *Talanta* **1991**, *38* (10), 1107–1109.

(18) Uno, T.; Okumura, K.; Kuroda, Y. *J. Org. Chem.* **1981**, *46* (16), 3175–3178.

(19) Zang, X.; Zhang, G.; Wang, C.; Wang, Z. *Se Pu Chin. J. Chromatogr.* **2015**, *33* (2), 103–111.

(20) Karlsson, B. C. G.; Olsson, G. D.; Friedman, R.; Rosengren, A. M.; Henschel, H.; Nicholls, I. A. *J. Phys. Chem. B* **2013**, *117* (8), 2384–2395.

(21) Rosengren, A. M.; Karlsson, B. C. G. *Biochem. Biophys. Res. Commun.* **2011**, *407* (2), 318–320.

1.3 References

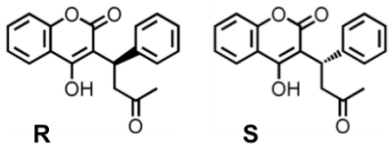

Figure 1. Warfarin enantiomers

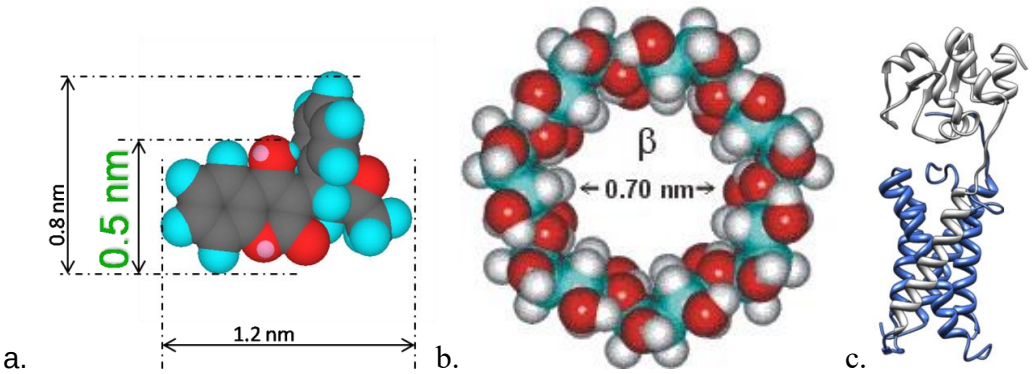

a. b. c.

Figure 2. (a) Warfarin dimensions; Binding scaffolds. (b.) Cyclodextrin and (c.) Vitamin K epoxide reductase (a) *Synechococcus sp*. (PDB: 3KP9).

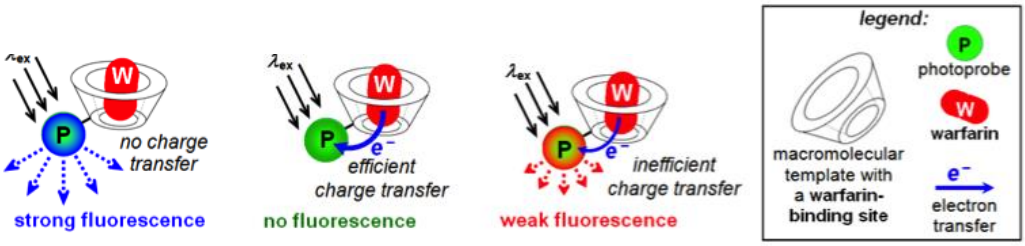

Figure 3. Fluorescent Fingerprint Sensing with a mixture of macromolecular sensors labeled with photoprobes fluorescing with different colors, and undergoing charge transfer with different efficiency. The quenching pattern of the differently colored fluorophores will depends on the oxidation potential of warfarin.

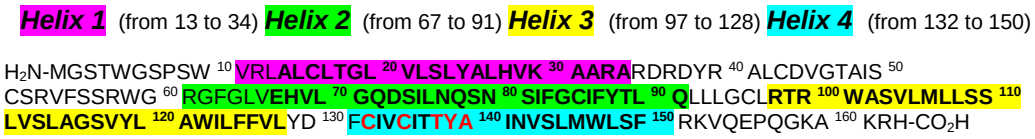

Figure 4. VKORC1 Sequence.

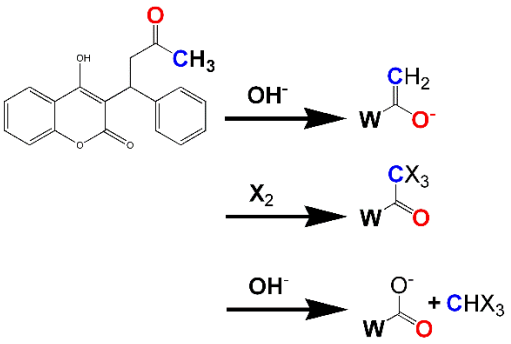

Figure 5. Haloform Reaction

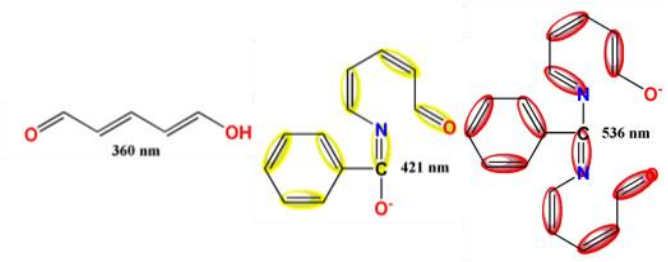

Figure 6. Fujiwara chromophores A/B/C

Chapter 2

Fluorescence Enhancement for Warfarin Sensing

CHAPTER 2: Inclusion Complexation of Warfarin with β-Cyclodextrin

Fluorescence Enhancement of Warfarin Induced by Interaction with β-Cyclodextrin

Introduction:

Warfarin is the most common agent used for control and prevention of venous as well as arterial thromboembolism (blood clots). In aqueous media, warfarin forms inclusion complexes with a family of cyclic oligosaccharides, α, β, γ-cyclodextrins (CD). The formation of these complexes results in enhancement of the fluorescence of warfarin. Such spectroscopic changes offer a venue for the development of bioanalytical methodologies for warfarin quantification in biological liquids. I have characterized the photophysical properties of warfarin in solvents with varying polarity and viscosity. The fluorescence quantum yield of warfarin correlated: (1) strongly with the solvent viscosity ($R = 0.979$) and (2) weakly with the solvent polarity ($R = 0.118$). These finding indicate that it is the change in viscosity, rather than the change in polarity, of the microenvironment that causes the fluorescence enhancement of warfarin upon binding to β-cyclodextrin. Utilizing the observed fluorescence enhancement in fluorescence titration measurements, the binding constants of warfarin to β-cyclodextrin were obtained (2.6×10^2 M^{-1}-3.7×10^2 M^{-1}). Using multivariable linear analysis, we extracted the stoichiometry of warfarin-β-cyclodextrin interaction (1:1).

2.1 Introduction

This chapter describes the characterization of the photophysical properties of an acidic anticoagulant, 4-Hydroxy-3-(3-oxo-1-phenylbutyl)coumarin (pKa = 5.1),[1] also known as warfarin (Scheme 1), in solvents with different polarities and viscosities. It was observed that an increase in the viscosity of the solvent media causes an increase in the fluorescence quantum yield of warfarin. The quantum yield of warfarin also increases upon binding to β-cyclodextrin. My finding suggests that it is the change in the viscosity, rather than the change in polarity, of the microenvironment of warfarin that causes the fluorescence enhancement upon its interaction with β-cyclodextrin. The Federal Drug Administration estimates that the coumarin derivative, warfarin (COUMADIN®) is prescribed to approximately 2 million new patients annually to prevent myocardial infarctions and hemorrhagic or ischemic stroke.[2] The clinical significance of warfarin lies in it ability to act as a potent anticoagulant. The synthetic pathway of hepatic vitamin-K dependent clotting factors (II, VII, IX, X) and hepatic proteins (C, S) is interrupted by warfarin-induced inhibition of vitamin K_1 epoxide regeneration, preventing coagulation.[3] Complications arising from warfarin therapy are categorized into two subgroups: hemorrhagic and non-hemorrhagic side effects, which include internal bleeding and skin necrosis, respectively.[4–7] Optimal dosage of warfarin varies for different individuals due to factors such as age, genetics, diet and medications taken concurrently.[2,8–10] Warfarin is a medication with a narrow therapeutic index (NTI) that requires close monitoring to prevent thromboembolic complications attributed to over- and under anticoagulation.[11]

According to the Federal Drug Administration, warfarin is the second largest cause of emergency room visits arising from drug complications annually, after insulin.[12] Currently, the clotting activity of warfarin in individual patients is estimated using a prothrombin-time (PT) test. The patients PT result is compared to an International Normalized Ratio (INR), derived from individuals in good health, which tends to be semi-qualitative.[2] The possible complications, coupled with the annual increase in the number of patients to whom warfarin therapeutics are prescribed, warrants development of an assay that will facilitate fast, accurate and quantitative monitoring of such NTI medications. It had been previously seen suggested that the formation of warfarin-cyclodextrin inclusion complex, causing fluorescence enhancement, offers a handle for Biosensing of this somewhat hydrophobic medication.[13–15] Driven by hydrophobic interactions, small molecules, including warfarin, tend to bind to β-cyclodextrin, which has a hydrophobic cavity, ~0.70 nm wide (Scheme 2).[1,6,16–25] The formation of inclusion complex with β-cyclodextrin results in fluorescence enhancement and increased solubility of warfarin.[21] The reported values for the binding constants between warfarin and β-cyclodextrin range from 00.8 M^{-1} to 633 M^{-1}.[14,18,21,25–29] Although it has not been proven definitively, the assumed stoichiometry for the binding between warfarin and β-cyclodextrin is 1:1. This chapter highlights my investigations into the solvent dependence of absorption and fluorescence properties of warfarin (as a racemic mixture) in order to gain understanding of the causes of emission enhancement that is observed upon binding of warfarin to cyclodextrins. To analyze the stoichiometry of interaction between warfarin and cyclodextrins, a two-variable model was developed, based on a one-variable

methodologies that the Vullev lab had previously adopted for investigation of aggregation equilibria of photoprobes and polypeptides.[30,31]

2.2 Results and Discussion

2.2.1 Solvent dependence of warfarin fluorescence. Valente et al.[32,33] described the dependence of isomeric ratios of warfarin in solution, as related to polarity, pH and redox properties of individual solvents. While for aqueous solution at neutral pH, the predominant tautomer of warfarin is its open form (Scheme 1), in alkaline (low dielectric constant) solutions, the hemiketal isomer predominates. Karlsson et al.[34] assigned characteristic peaks in the absorption spectra to each of the tautomeric forms. The peak present at $\lambda = 310$ nm is representative of the open side chain isomer, whereas, the cyclic hemiketal peak appears at $\lambda = 280$ nm. My work was aimed to further investigate the dependence of fluorescence enhancement of warfarin, attributed not only to the solvent polarity, but also the media viscosity (Table 1).

A series of protic solvents (water and alcohols) with various polarities and viscosities for spectroscopic studies. Peaks corresponding to the non-charged isomers of warfarin with an open side chain ($\lambda = 310$ nm) and cyclic hemiketal ($\lambda = 280$ nm) are seen in the absorption spectra for solvents with different polarity and viscosity (Figure 1). While the viscosity of the solvent did not affect the ratio between the 280 nm and 310 nm absorption peaks (Figure 1a, blue lines), decrease in the solvent polarity appeared to favor the cyclic hemiketal tautomer (see strong absorption peak at 280 nm for 1-butanol, Figure 1a).

For characterization of the emission properties of warfarin, we selectively excited the open form at 310 nm. Although the emission curves were identical for all solvents, the fluorescence spectra of warfarin showed a marked intensity increase in glycerol and ethylene glycol in comparison to the other solvents (Figure 1b). While the quantum yield of warfarin, Φ, manifested no (or negligible) correlation with the solvent polarity (Figure 2a), Φ correlated strongly with the dynamic viscosity of the solvent media (Figure 2b). My results are in excellent agreement with observed quantum yield enhancement in a sucrose gradient.[35,36] These finding suggest that the increase in the viscosity of the environment considerably suppresses the vibrionic modes that provide pathways of non-radiative transitions between the excited and ground states of warfarin. As a result, the viscous solvents cause a decrease in the rates of the non-radiative decay processes and hence, overall increase in the emission quantum yield of warfarin.

2.2.2 Temperature dependence of warfarin fluorescence

Increase in the temperature can affect the fluorescence quantum yield of warfarin, Φ, in three distinct manners: (i) Thermal excitation to upper vibrational levels of the lowest excited state can increase the number of pathways for non-radiative decay and hence, decrease Φ. (ii.) A temperature-induced shift in the equilibrium from the closed to open for of warfarin (Scheme 1), as evident from the decrease in absorption in the 280 nm region with an increase in temperature (Figure 3), can alter Φ. (iii.) A temperature – induced decrease in the viscosity of the solvent media leads to a decrease in Φ (Figures 4

and 5). Our finding, however, suggests that the latter, (iii.), has prevalent effect on the temperature dependence of the fluorescence properties of warfarin.

The most prevalent temperature-induced changes in the fluorescence quantum yield of warfarin were observed for glycerol and ethylene glycol, while for water and methanol Φ did not manifest significant temperature dependence (Figure 5a). The viscosity of glycerol, for example, decreases considerably with an increase in temperature: i.e,. the dynamic viscosity of glycerol, determined for 10°C and for 70°C, is 3900 cP and 50.60 cP, respectively.[37] The dynamic viscosities of water and methanol, on the other hand, remain relatively low within the investigated temperature range and their temperature dependence is not as dramatic as the temperature range and the temperature observed for glycerol. The dynamic viscosity of water is 1.30 cP and 0.406 cP for 10°C and 70°C, respectively[38] and the dynamic viscosity of methanol is 0.581 cP and 0.398 cP for 20°C and 50°C, respectively.[39,40] These findings, therefore, suggest that the observed temperature dependence of the fluorescence quantum yield of warfarin is predominantly induced by changes in the viscosity of the media resultant from thermal alterations.

2.2.3 Warfarin-β-Cyclodextrin interaction

To examine the binding of warfarin to β-cyclodextrin, we conducted two-dimensional fluorescence titrations at four different warfarin concentrations varying the amount of β-cyclodextrin (Figure 6). Addition of β-Cyclodextrin to aqueous solutions of warfarin caused slight blue shifts without changing the shape of the measured absorption spectra

(Figure 6a). Warfarin-β-cyclodextrin interaction did not result in an appearance of an absorption peak at ~280 nm (as observed, for example, for 1-butnaol, Figure 1a), suggesting that warfarin exists predominantly in its open for when bound to β-cyclodextrin. Despite the hydrophobicity of the cavity of the cyclic carbohydrate, steric hinderence is probably the main cause for warfarin to remain in its open and more extended form in comparison with the cyclic form observed for hydrophobic media (Scheme1).

For all warfarin concentrations (we used 5, 20, 50 and 100 uM warfarin), the addition of β-cyclodextrin caused less than 10% change in absorption at 310 nm (Figure 6a). When exciting at 310 nm, however, we observed about five-fold increase in the fluorescence intensity of warfarin upon addition of β-cyclodextrin in excess (Figure 6b). Because of its limited solubility in water, the maximum concentration of β-cyclodextrin we attained was 15 mM. We ascribe the observed enhancement of the fluorescence of warfarin upon binding to β-cyclodextrin to the increased effective viscosity of the microenvironment inside the hydrophobic cavity of the cyclic carbohydrate: i.e., β-cyclodextrin constrains molecular motion of warfarin that can lead to non-radiative decay. [I should elaborate on this point … see mechanism explanation]

From sigmoidal plots of warfarin fluorescence quantum yield, Φ, vs. the concentration of β-cyclodextrin in logarithmic scale (Figure 6c), we extracted values for the warfarin-β-cyclodextrin binding constant: 2.6 x 10^2 M^{-1}, 2.5 x10^2 M^{-1}, 3.0 x10^2 M^{-1} and 3.7 x10^2 M^{-1} for titrations of 5μM, 20μM, 50μM and 100μM warfarin, respectively (assuming 1:1 binding stoichiometry). Extrapolation to infinity β-cyclodextrin

concentration yielded the fluorescence quantum yield for warfarin bound to β-cyclodextrin. Similar to the binding constant, the fluorescence quantum yield for "infinite" cyclodextrin concentration manifested small increases with the increase in the concentration of the titrated warfarin: 0.056 ± 0.003, 0.060 ± 0.002, 0.067 ± 0.004 and 0.064 ± 0.010 for titration of 5μM, 20μM, 50μM and 100μM warfarin, respectively. These quantum yield values are smaller only than the warfarin quantum yield for glycerol (Table 1). Therefore, we can estimate the effective viscosity of the β-cyclodextrin cavity for warfarin is between about 18 and 47 cP.

Because the quantum yield and the binding constant are concentration independent, the obtained values should be identical or have a scatter behavior; i.e., they should not manifest correlation with the warfarin concentration. Although the observed variations in the obtained values of the binding constant might not appear significant and can be readily ascribed to experimental uncertainty, the enormous discrepancies for the binding affinity of warfarin to cyclodextrin that are previously reported,[14,18,21,25–29] make our own observations somewhat alarming.

The racemic nature of the warfarin used for this study, can provide a plausible reason for the observed concentration dependence of the binding constants and the quantum yield values. While the warfarin is a 1:1 mixture of R and S enantiomers, β-cyclodextrin is enantiomerically pure. In our current analysis, as well as in previously published binding studies[13–15,21,22,26,27,41] the racemic mixture is treated as a single compound that underlines an assumption that R and S enantiomers have the same binding constant for β-cyclodextrin and identical quantum yields when bound to β-cyclodextrin,

however, will result in discrimination between the binding properties of R and S warfarin, as well as between the rigidity of the microenvironment for R and S enantiomers in the bound complex.[28] Therefore, the titration measurements have characteristics of competitive binding between the two enantiomers and the cyclodextrin-bound R and S warfarin should have different fluorescence quantum yields.

2.3 Discussion: Stoichiometry of warfarin-β-cyclodextrin binding

The relatively small differences between the binding constants and the quantum yields for the different warfarin concentrations, however, indicate that the enantioselectivity of β-cyclodextrin toward either of the warfarin enantiomers is not significant. (For 20-fold increase in the estimated values for the binding constants and less than a 1.2-fold change in the quantum yield of the bound fluorophore). Therefore, we can adopt a two-variable one-step model to estimate the binding stoichiometry between warfarin and β-cyclodextrin.

From a power-law relationship, we developed a linear expression modeling the assumption that the observed fluorescence enhancement is based on *n* molecules of warfarin (W) bound with *m* molecules of cyclodextrin (CD):

$$\boldsymbol{nW + mCD \leftrightarrow CD_mW_n}$$

The binding constant, K, for this process is:

$$\boldsymbol{K = \frac{CD_mW_n}{[W]^n[CD]^m}}$$

Where [W], [CD] and [CD_mW_n] are the equilibrium concentrations of warfarin, cyclodextrin and the warfarin-cyclodextrin complex, respectively.

The total concentration of warfarin, C_w, and the total concentration through the whole titration are expressed as:

$$C_W = [W] + n[CD_mW_n]$$

$$C_{CD} = [CD] + m[CD_mW_n]$$

The measured quantum yield for a mixture of free and cyclodextrin-bound warfarin, can be expressed as the weighted sum of the quantum yield of warfarin in buffer, Φ_0 (i.e., $C_{CD} = 0$), and the quantum yield of cyclodextrin-bound warfarin, Φ_∞ (i.e., $C_{CD} = \infty$):

$$\Phi = \frac{[W]}{C_W}\Phi_0 + n\frac{CD_mW_n}{C_W}\Phi_\infty$$

Combining Eq. 2 to 4 produce a power-law expression, which yields a linear relationship between the logarithms of the measured quantities with the stoichiometric parameters, n and m, as proportionality coefficients: [show formula derivation … long form]

$$\lg\big(C_W(\Phi \quad - \Phi_0)\big)$$

$$= m\, lg(C_{CD}) + n\, lg(C_W(\Phi_\infty - \Phi \quad)) + \lg(nK) + (1-n)\lg(\Phi \quad - \Phi_0))$$

Plotting in a three-dimensional space $\lg\big(C_W(\Phi \quad - \Phi_0)\big)$ vs. $lg(C_{CD})$ and $lg(C_W(\Phi_\infty - \Phi \quad))$ will produce a plane with slopes along the x- and y-axes equal to m and n, respectively. The intercept of the place with the z-axis will yield $\lg(nK) + (1 - n)\lg(\Phi \quad - \Phi_0)$.

To derive Eq. 5, we needed to simplify Eq. 3b to $C_{CD} \approx [CD]$, i.e., assuming that the total concentration of cyclodextrin considerably exceeds the total concentration of

warfarin. For this two variable linear analysis, therefore, we selected the data, in which Ccd ranges between 1 and 10 mM. A plot of $lg(C_W(\Phi_\infty - \Phi\ ))$ vs. $lg(C_{CD})$ and $lg(C_W(\Phi_\infty - \Phi\ ))$, indeed resulted in a tilted plane (Figure 7a). A linear two parameter fit, i.e., f(x,y) = Z = mx + ny + z0, yielded the slopes of this plane: m = 0.847 and n = 1.02 (Figure 7b,c). Both coefficients, m and n, can be approximated to 1 (the closest integer number) confirming the 1:1 stoichiometry that has been assumed for interaction between warfarin and β-cyclodextrin.

The stoichiometry coefficient for β-cyclodextrin, m, however, appears to be underestimated. There are three possible reasons for such an underestimation of m: (i.) Eq. 5 assumes that $C_W \ll C_{CD}$. For warfarin concentration of 100 uM, the smallest CD concentration was only ten times larger, i.e., 1mM. (ii.) We assumed that the binding properties of the R and S warfarin to β-cyclodextrin are similar. Taking under consideration the molecular size of warfarin and the size of the β-cyclodextrin opening (Scheme 2), it is most likely that the binding ratios for the R and S enantiomers with β-cyclodextrin are identical. Even if the binding ratios are 1:1 for R and S warfarin (Eq. 2), a difference in the binding constants for the two enantiomers may result in non-integer values of n and/or m (Eq. 5). (iii.) The coefficient m is quite sensitive to the value of Φ_∞: i.e., larger Φ_∞ values tend to produce smaller m. The values of Φ_∞ were estimated from extrapolation to infinity CD concentration. Solubility limitations did not allow us to attain sufficiently high cyclodextrin concentrations at which warfarin is quantitatively bound to the β-cyclodextrin that would have considerably improved the certainty of the obtained values for Φ_∞.

2.4 Conclusions

Although the absorption properties of warfarin show dependence on solvent polarity, its fluorescence quantum yield strongly correlates with the viscosity of the media. Therefore, the observed fluorescence enhancement of warfarin, upon binding to β-cyclodextrin, results from the increased effective viscosity of the microenvironment within the β-cyclodextrin cavity. We believe that the model for the linear two-variable analysis, which we developed to confirm the 1:1 stoichiometry of warfarin-β-cyclodextrin interaction, is universally applicable for a broad range of one-step binding proesses.

2.5 Experimental

Reagents

Racemic warfarin (4-Hydroxy-3-(3-oxo-1-phenylbutyl) coumarin, min 98% was obtained from Sigma-Aldrich (St. Louis, MO). The cyclic oligosaccharide, β-cyclodextrin (min, 98%) was obtained from Sigma –Aldrich (St. Louis, MO). Quinine sulfate was obtained from Sigma-Aldrich (St. Louis, MO). Water used in the solutions was Millipore grade (Millipore, Bedford, MA). Organic solvents Ethanol, 1-Butanol, Ethylene Glycol and Glycerol were of spectroscopic grade, obtained from Sigma-Aldrich (St. Louis, MO). Organic solvents Methanol and 1-Propanol were of spectroscopic grade obtained from Fluka (St. Louis, MO). The buffer used was phosphate-buffered saline (PBS, pH ~7.4, 10 mM sodium phosphate) obtained from Sigma-Aldrich (St. Louis, MO).

Instrumentation

Fluorescence spectra measurements were scanned at room temperature, between 300 and 550 nm on a Jobin-Yvon HORIBA Fluorolog-3-22 fluorimeter. UV/Visible absorption spectra measurements were scanned at room temperature, between 200 and 500 nm on a Varian Cary spectrophotometer. Quartz cuvettes (1.0 cm, 3.0 mL) were used in all spectroscopic measurements, obtained from Starna Cells Inc (Atascadero, CA).

Absorption/fluorescence spectroscopy

All solutions were prepared using 0.01 M phosphate buffered saline at pH ~7.4. Each titration set had a fixed warfarin concentration (5 μM, 20 μM, 50 μM, 100 μM), obtained from fresh 10 mM warfarin stock solution dissolved in methanol. Each experimental solution of β-cyclodextrin (10 μM, 20 μM, **50** μM, 150 μM, 250 μM, 500 μM, 750 μM, 1 mM, 1.5 mM, 2 mM, 3.5 mM, 5 mM, 10mM and 15 mM) was obtained from a 15mM stock solution dissolved in phosphate-bufered saline. To avoid dilution correction, fresh solutions of CW + CCD + PBS were made fresh for every measurments.

Steady-state fluorescence and quantum yield measurements

The fluorescence quantum yield (Φ) was performed using quinine sulfate as a standard reference compound at the excitation wavelength 310 nm in 0.1 M H2SO4 (20 μM, ΦF =

0.577).[42,43] The ΦF for warfarin in the different solvents was calculated according to Eq. 6.[44] ΦR is the quantum yield of the reference standard using, IR,W represents the fluorescence integral of the emission between 300 and 550 nm, ARW are the absorbance's at the excitation wavelengths, and finally *n* represents the refractive indices for the standard and the experimental solvent.

$$\Phi_W = \Phi_R \left(\frac{I_W}{I_R}\right)\left(\frac{1-10^{-A_R}}{1-10^{-A_W}}\right)\left(\frac{n_W}{n_R}\right)^2$$

Steady-state titration studies

Aliquots of the 10 mM warfarin stock (5 μM = 1.5 μL, 20 μM = 6.0 μL, 50 μM = 15.0 μL, 100 μM = 30.0 μL) were added to volumes of β-cyclodextrin (10 μM = 2.0 μL, 20 μM = 4.0 μL, 50 μM = 10.0 μL, 150 μM = 30.0 μL, 250 μM = 50.0 μL 500 μM = 100.0 μL, 750 μM = 150.0 μL, 1 mM = 200 μL, 1.5 mM = 300 μL, 2 mM = 400 μL, 3.5 mM = 700 μL, 5 mM = 1,000 μL, 10 mM = 2000 μL and 15 mM = 3000 μL), brought to a final olume of VF = 3 mL with phosphate buffered solution. All titration studies were done using an excitation wavelength of 310 nm. The fluorescence emission spectra were obtained after mixing and one minute incubation.

Table 1: Quantum Yield, Φ_F Determinations: Dielectric Constant ε, Fluorescence Quantum Yield Φ

Solvents	Φ[a]	ε[b]	η / cP[b,c]
1-Butanol	0.042	17.84	2.45
Ethanol	0.027	25.30	1.07
Ethylene Glycol	0.037	41.40	16.06
Glycerol	0.104	46.53	934.00
Methanol	0.017	33.00	0.54
1-Propanol	0.021	20.80	1.95
Water	0.012	80.10	0.89

[a] λ_{ex} = 310nm

[b] David R. Lide, ed., CRC Handbook of Chemistry and Physics, 2007, (88th Edition), Taylor and Francis (22)

[c] η = Dynamic viscosity of solvents

2.7 Schemes

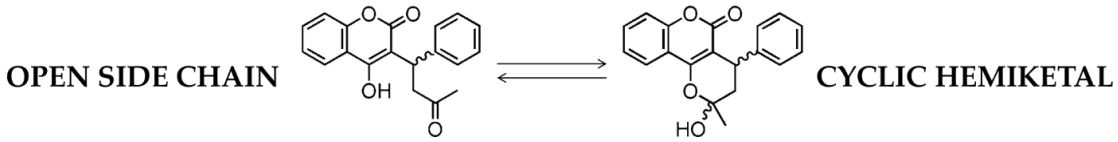

Scheme 2-1
Equilibrium between a closed and open form of warfarin

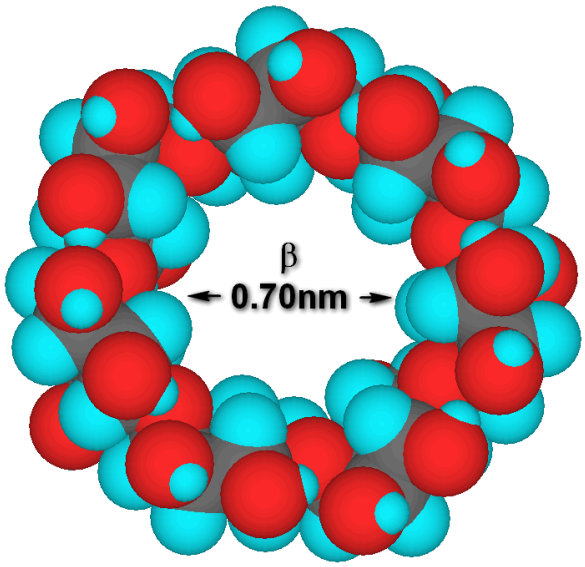

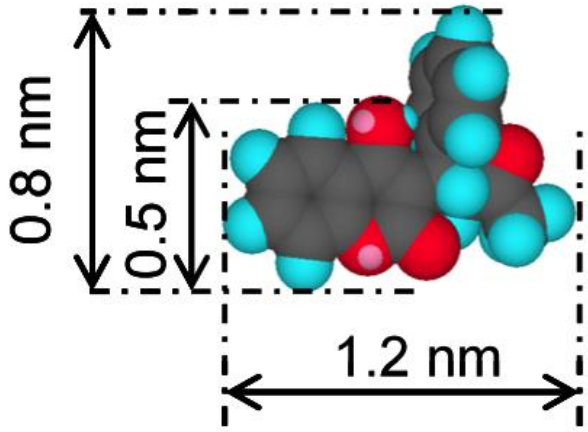

Scheme 2-2
Space-filling models of β-cyclodextrin (β-CD) and warfarin (*W*) with corresponding dimensions

2.8 Figures

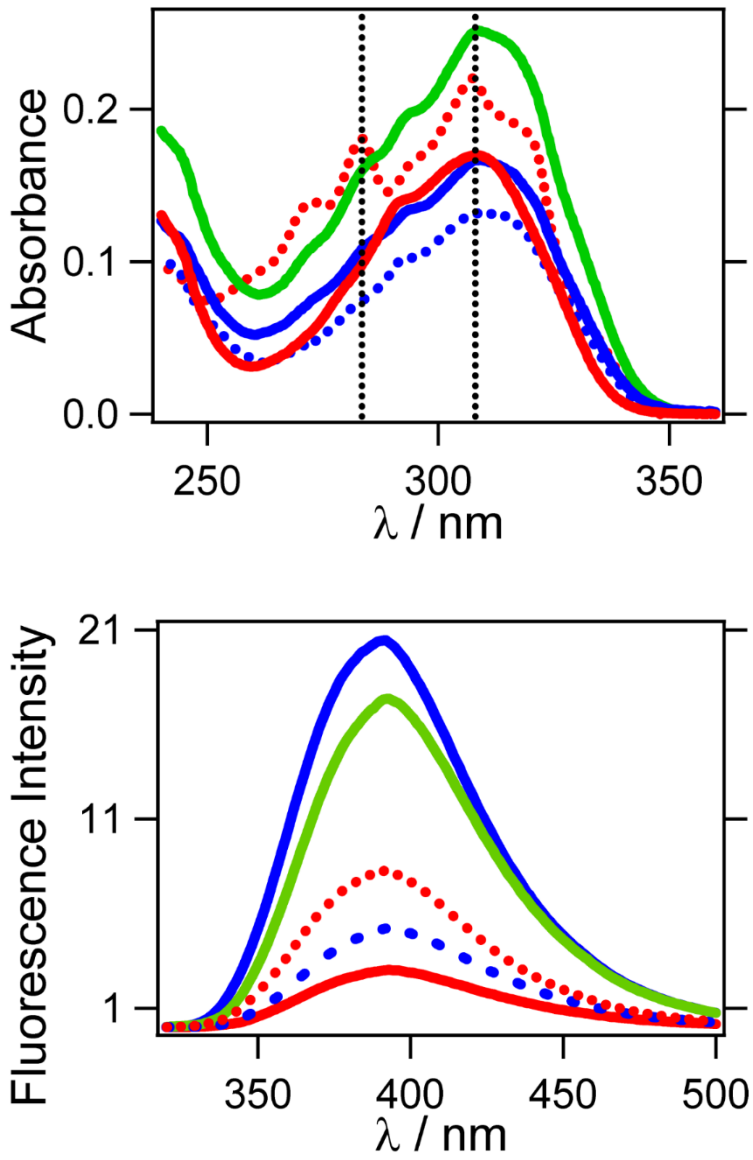

Figure 2-1
(a) Absorption and (b) fluorescence spectra (λ_{ex} = 310 nm) of warfarin (20 μM) for solvents with various polarity (red lines) and viscosity (blue lines); red solid = water (most polar), red dashed = 1-butanol (least polar), blue solid = glycerol (most viscous), blue dashed = methanol (least viscous), green solid = ethylene glycol.

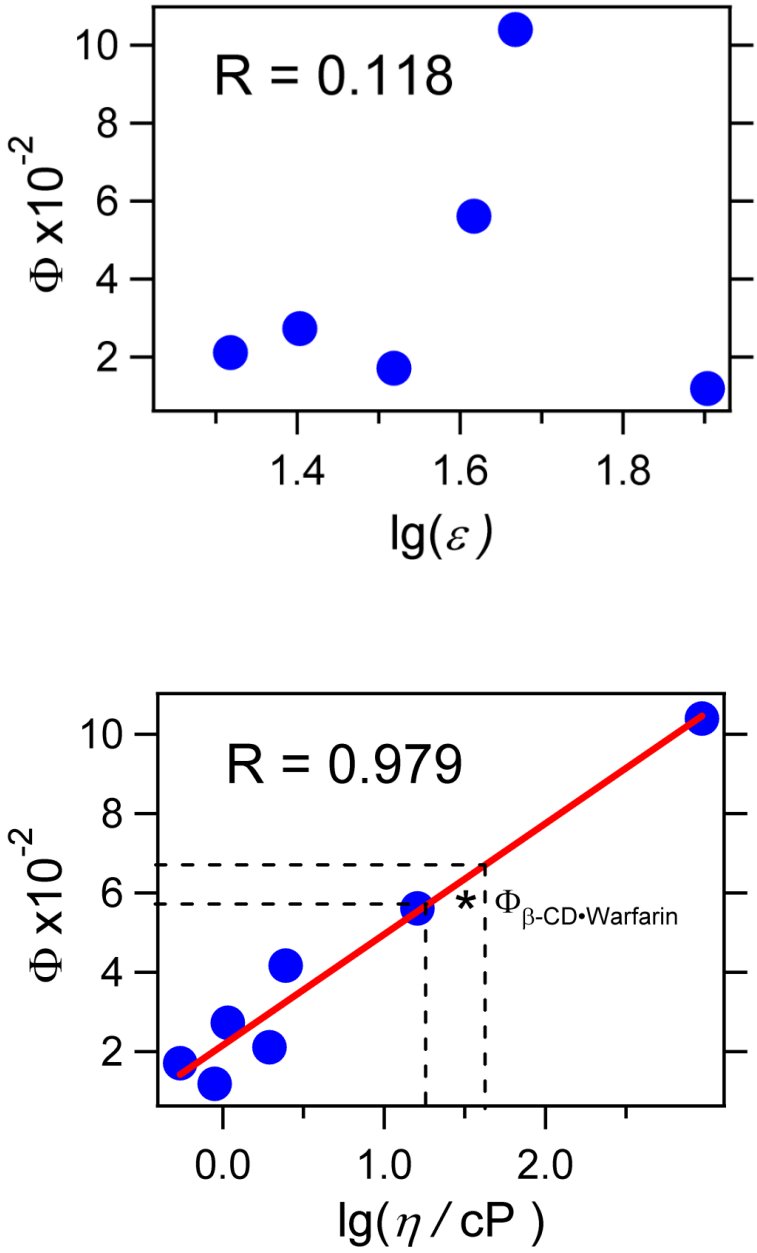

Figure 2-2
Correlation analyses between the warfarin fluorescence quantum yield, Φ, and: (a) the solvent polarity (expressed logarithmically in terms of the solvent static dielectric constant, ε), and (b) the solvent viscosity (expressed logarimically in terms of the solvent dynamic viscosity, η).

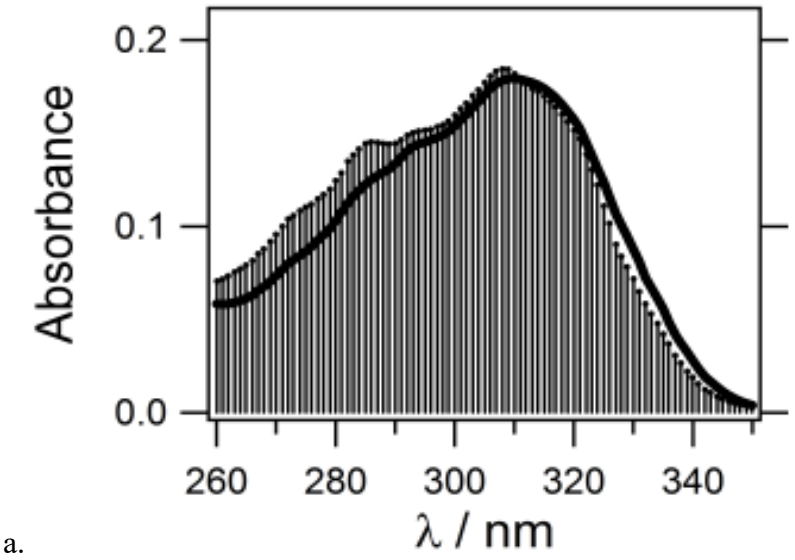

a.

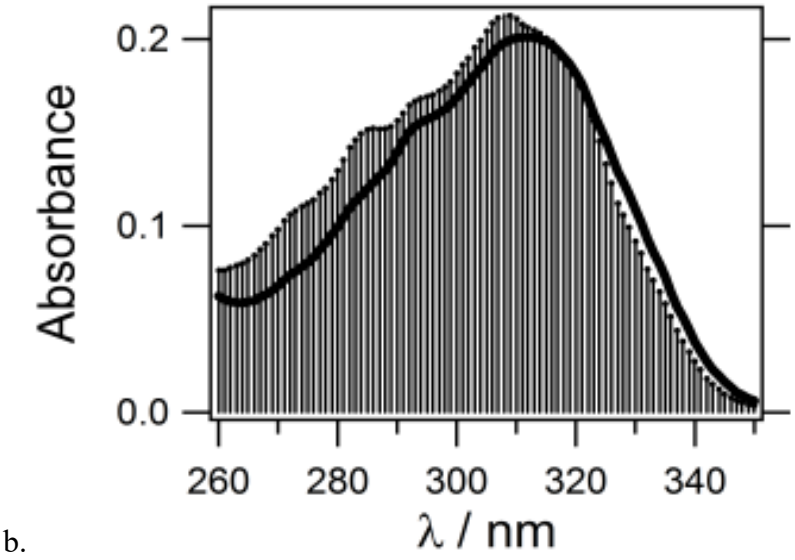

b.

Figure 2-3
Temperature dependence of the absorption spectra of warfarin (20 μM) for (a) glycerol; (b) ethylene glycol; (c) water; and (d) methanol.
Shaded spectra for all solvents are acquired at 10°C. The solid lines correspond to spectra acquired at 70°C for all solvents except methanol, for which the solid-line spectrum corresponds to acquisition at 62°C.

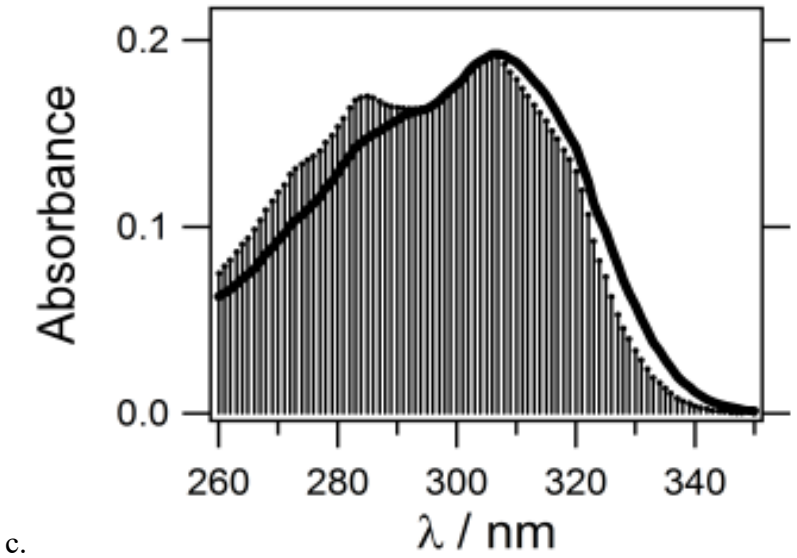

c.

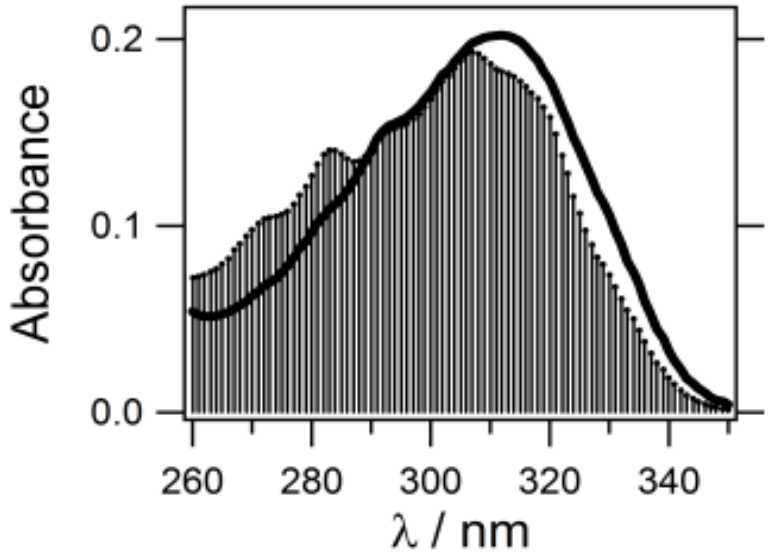

d.

Figure 2-3
Temperature dependence of the absorption spectra of warfarin (20 μM) for (a) glycerol; (b) ethylene glycol; (c) water; and (d) methanol.
Shaded spectra for all solvents are acquired at 10°C. The solid lines correspond to spectra acquired at 70°C for all solvents except methanol, for which the solid-line spectrum corresponds to acquisition at 62°C.

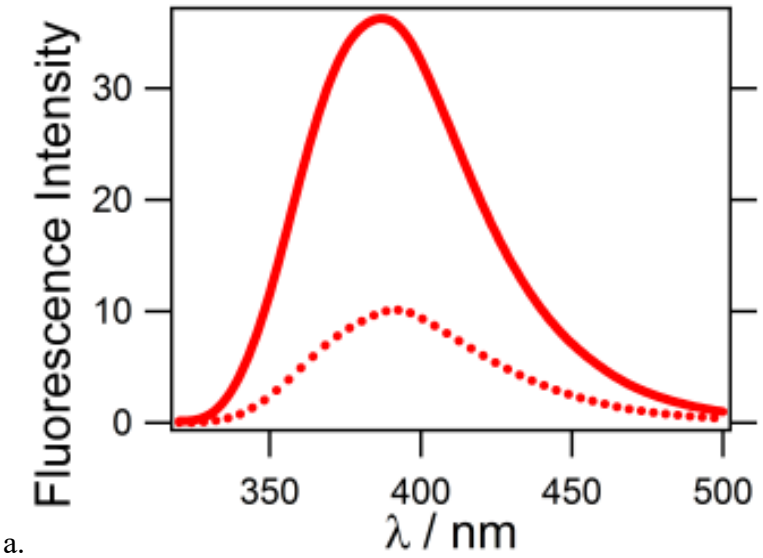

a.

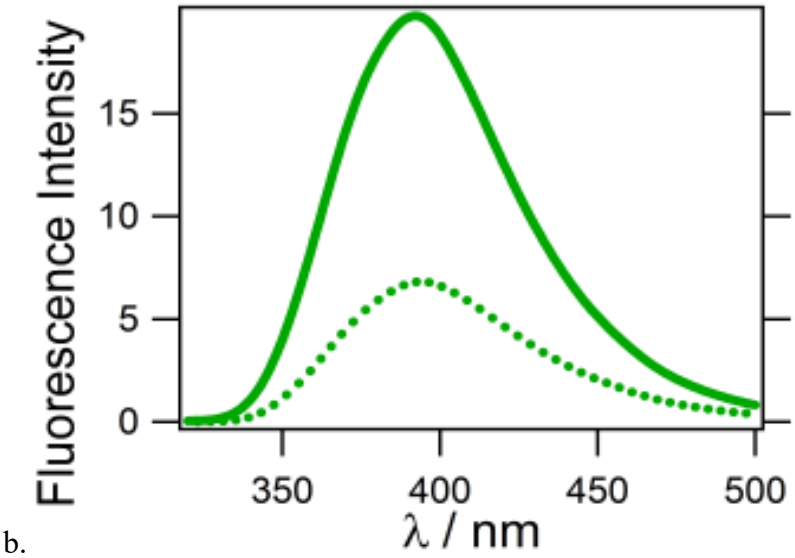

b.

Figure 2-4
Temperature dependence of the fluorescence spectra of warfarin (20 μM, λ_{ex} = 310 nm) for (a) glycerol; (b) ethylene glycol; (c) water; and (d) methanol.
The solid lines correspond to spectra acquired at 70°C for all solvents except methanol, for which the solid-line spectrum corresponds to acquisition at 62°C.

c.

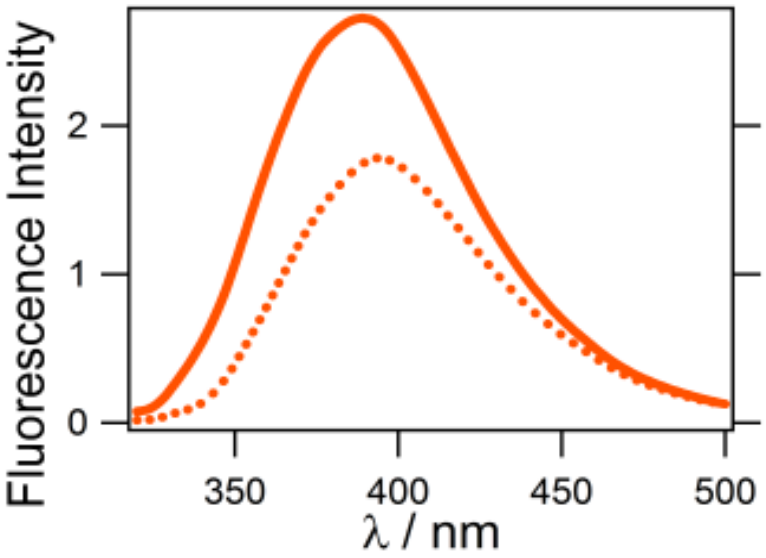

d.

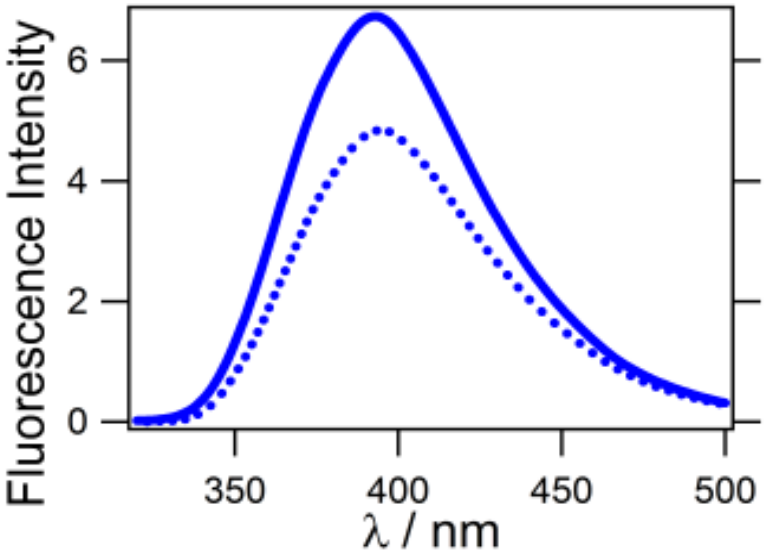

Figure 2-4
Temperature dependence of the fluorescence spectra of warfarin (20 μM, λ_{ex} = 310 nm) for (a) glycerol; (b) ethylene glycol; (c) water; and (d) methanol.
The solid lines correspond to spectra acquired at 70°C for all solvents except methanol, for which the solid-line spectrum corresponds to acquisition at 62°C.

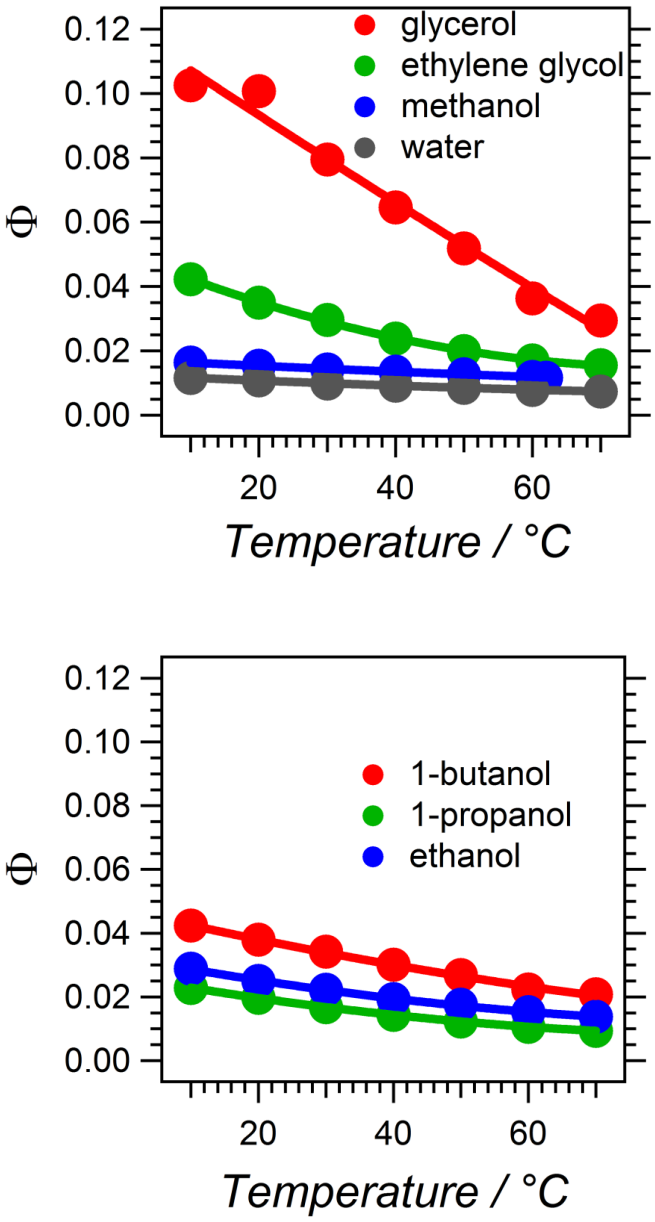

Figure 2-5
Temperature dependence of the fluorescence quantum yield of warfarin, Φ, for various protic solvents.

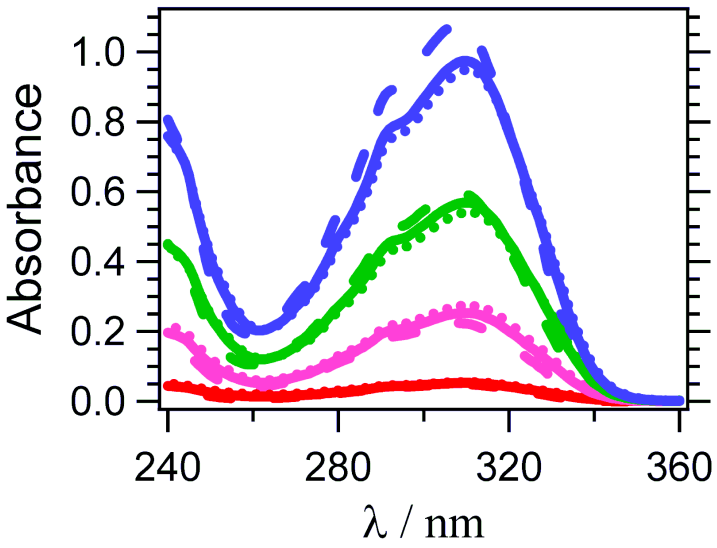

a.

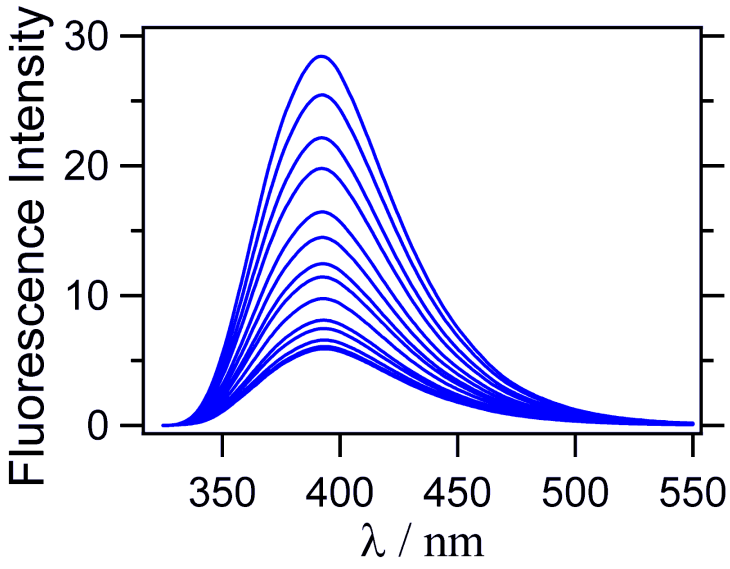

b.

Figure 2-6
(a) Absorption Spectra [5 (red), 20 (pink, 50 (green), 100 μM (blue) Warfarin/0 (dotted), 5 (solid), 10 (dashed) mM β-CD]. (b) Fluorescence enhancement of 100 μM Warfarin over all β-cyclodextrin concentrations (10-15 mM). (c) Binding constant extraction.

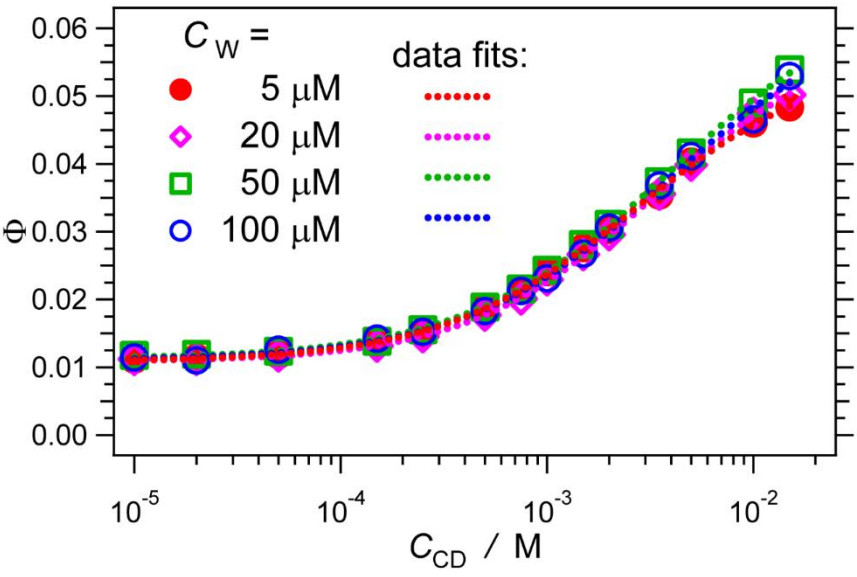

c.

Figure 2-6
(a) Absorption Spectra [5 (red), 20 (pink, 50 (green), 100 μM (blue) Warfarin/0 (dotted), 5 (solid), 10 (dashed) mM β-CD]. (b) Fluorescence enhancement of 100 μM Warfarin over all β-cyclodextrin concentrations (10-15 mM). (c) Binding constant extraction.

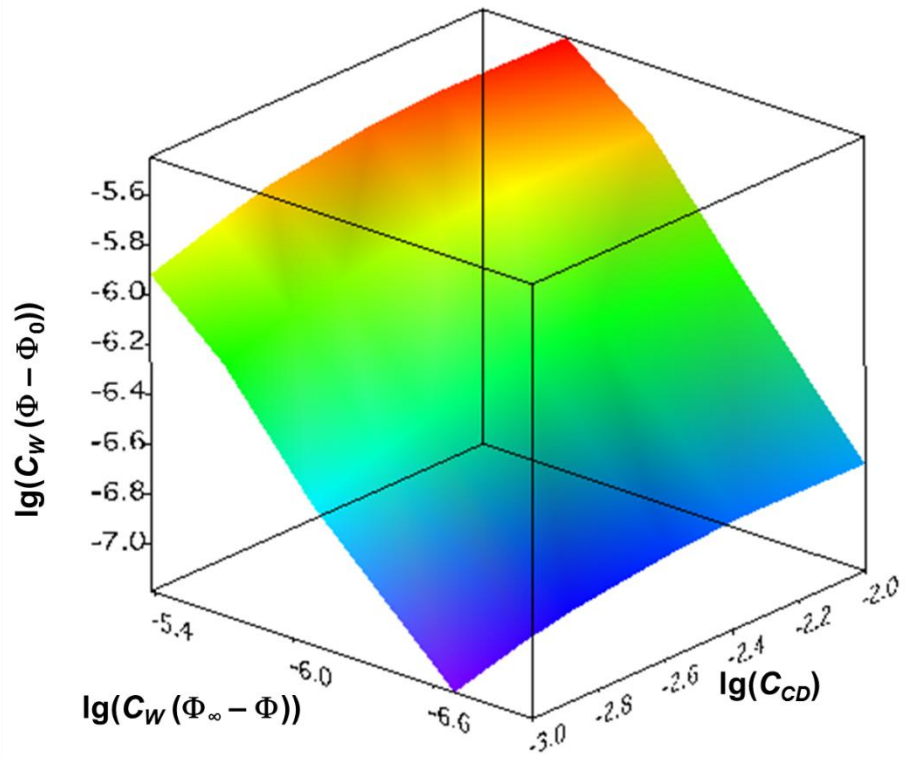

a.

Figure 2-7
Two-variable linear analysis of fluorescence titration of warfarin with β-cyclodextrin. (a) Surface plot of the data represented with linearly dependent logarithmic quantities (Eq. 5). (b) Slices of the surface plot along $\lg(C_w(\Phi_\infty - \Phi))$. Because the data points from the same slice have different values for Φ, the linear appear curved. (c) Slices of the surface plot at different values of C_{CD}. The red circles represent the data points and the blue lines the linear fit.

b.

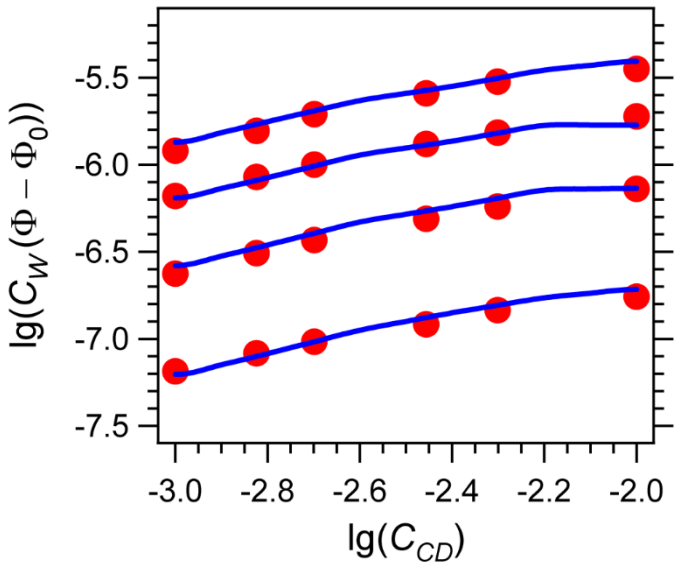

c.

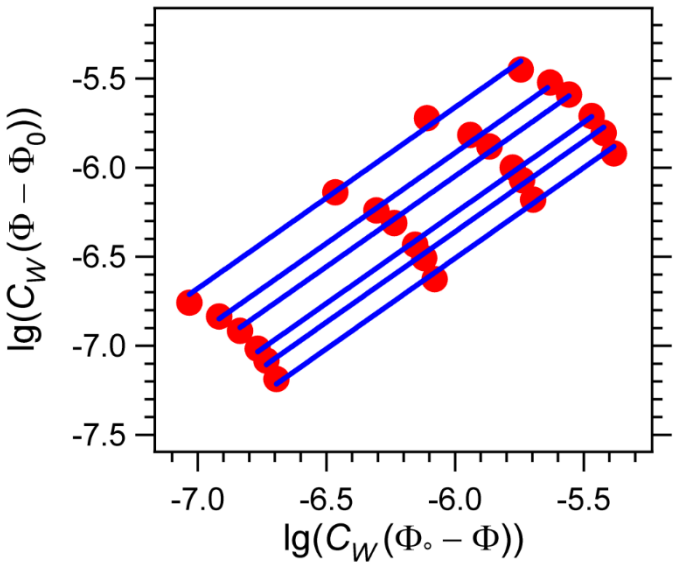

Figure 2-7
Two-variable linear analysis of fluorescence titration of warfarin with β-cyclodextrin. (a) Surface plot of the data represented with linearly dependent logarithmic quantities (Eq. 5). (b) Slices of the surface plot along $\lg(C_w(\Phi_\infty - \Phi))$. Because the data points from the same slice have different values for Φ, the linear appear curved. (c) Slices of the surface plot at different values of C_{CD}. The red circles represent the data points and the blue lines the linear fit.

References

1. Otagiri M, Fokkens JG, Hardee GE, Perrin JH. The interaction of some coumarin anticoagulants with beta-cyclodextrin in phosphate buffers. Pharmaceutica Acta Helvetiae 1978;53:241– 247.

2. Bristol-Meyers Squibb Company. COUMADIN Medication Guide. Princeton, NJ: Bristol-Meyers Squibb Company; 2007.

3. Park BK. Warfarin: metabolism and mode of action. Biochem Pharmacol. 1988;37:19–27.

4. Buller HR, Agnelli G, Hull RD. Hyers TM, Prins MH, Raskob GE. Antithrombotic therapy for venous thromboembolic disease: the seventh ACCP conference on antithrombotic and thrombolytic therapy. Chest. 2004;126(3 Suppl):401S–428S.

5. Cornett O, Lenore OC, Singh M, Malhotra S, Rosenbaum DM. Antithrombotic and thrombolytic therapy for ischemic stroke. Cardiol Clin. 2008;26:251–265.

6. Loftsson T, Brewster ME. Pharmaceutical applications of cyclodextrins. I. Drug solubilization and stabilization. J Pharm Sci. 1996;85:1017–1025.

7. Singer DE, Albers GW, Dalen JE, Fang MC, Go AS, Halperin JL, Lip GYH, Manning WJ. Antithrombotic therapy in atrial fibrillation: American college of chest physicians evidence-based clinical practice guidelines (8th ed). Chest. 2008;133(6 Suppl):546S–592S.

8. American Geriatric Society, CPC. The use of oral anticoagulants (warfarin) in older people. J Am Geriatr Soc. 2000;48: 224–227.

9. Herman D, Locatelli I, Grabnar I, Peternel P, Stegnar M, Mrhar A, Breskvar K, Dolzan V. Influence of CYP2C9 polymorphisms, demographic factors and concomitant drug therapy on warfarin metabolism and maintenance dose. Pharmacogenomics J. 2005;5:193–202.

10. Takahashi H, Wilkinson GR, Nutescu EA, Morita T, Ritchie MD, Scordo MG, Pengo V, Barban M, Padrini R, Ieiri I, Otsubo K, Kashima T, Kimura S, Kijima S, Echizen H. Different contributions of polymorphisms in VKORC1 and CYP2C9 to intraand inter-population differences in maintenance dose of warfarin in Japanese, Caucasians and African-Americans. Pharmacogenet Genomics. 2006;16:101–110. 11. Schulman S, Beyth RJ, Kearon C, Levine MN. Hemorrhagic complications of anticoagulant and thrombolytic treatment: American College of Chest Physicians evidence-based clinical practice guidelines (8th edition). Chest. 2008;133(6 Suppl): 257S–298S.

12. FDA News FDA Approves Updated Warfarin (Coumadin) Prescribing Information: New Genetic Information May Help Providers Improve Initial Dosing Estimates of the Anticoagulant for Individual Patients. Available at: http://www.fda.gov/bbs/ topics/news/2007/new01684.html.AQ2

13. Badia R, Diaz-Garcia ME. Cyclodextrin-based optosensor for the determination of warfarin in waters. J Agric Food Chem. 1999;47:4256–4260.

14. Marquez JC, Hernandez M, Garcia-Sanchez F. Enhanced spectrofluorimetric determination of the pesticide warfarin by means of the inclusion complex with beta-cyclodextrin. Analyst. 1990;115:1003–1005.

15. Tang LX, Rowell FJ. Rapid determination of warfarin by sequential injection analysis with cyclodextrin-enhanced fluorescence detection. Anal Lett. 1998;31:891–901.

16. Al-Hassan KA, Meetani MA, Said ZFM. Fluorescence probes as molecular weight detectors of polymers. J Fluoresc. 1998; 8:93–100.

17. Chen J, Ohnmacht CM, Hage DS. Characterization of drug interactions with soluble beta-cyclodextrin by high-performance affinity chromatography. J Chromatogr. 2004;1033:115–126.

18. Chen W, Chang C, Gilson MK. Calculation of cyclodextrin binding affinities: energy, entropy, and implications for drug design. Biophys J. 2004;87:3035–3049. 19. Dondon R, Fery-Forgues S. Inclusion complex of fluorescent 4-hydroxycoumarin derivatives with native b-Cyclodextrin: enhanced stabilization induced by the appended substituent. J Phys Chem B. 2001;105:10715–10722.

20. Hoshino M, Imamura M, Ikehara K, Hama Y. Fluorescence enhancement of benzene derivatives by forming inclusion complexes with b-cyclodextrin in aqueous solutions. J Phys Chem. 1981;85:1820–1823.

21. Lin SY, Yang JC. Inclusion complexation of warfarin with cyclodextrins to improve some pharmaceutical characteristics. Pharm Weekbl Sci Ed. 1986;8:223–228.

22. Otagiri M, Uekama K, Ikeda K. Inclusion complexes of betacylodextrin with tranquilizing drugs phenothiazines in aqueous solution. Chem Pharm Bull. 1975;23:188–195.

23. Sato Y, Suzuki Y. Optical resolution of drugs by cyclodextrin complexation. Chem Pharm Bull. 1985;33. AQ3

24. Wang E, Lian Z, Cai J. The crystal structure of the 1:1 inclusion complex of .beta.-cyclodextrin with benzamide. Carbohydr Res. 2007;342:767–771.

25. Zingone G, Rubessa F. Preformulation study of the inclusion complex warfarin-beta-cyclodextrin. Int J Pharm. 2005;291:3–10.

26. Ishiwata S, Kamiya M. Cyclodextrin inclusion effects on fluorescence and fluorimetric properties of the pesticide warfarin. Chemosphere. 1997;34:783–789. 27. Karadag O, Gok E, Serdar A. Inclusion complexation of warfarin with beta-cyclodextrins and its influence on absorption kinetics of warfarin in rat. J Inclus Phenom Mol Recogn Chem. 1995;20:23–32.

28. Karnik NA, Prankerd RJ, Perrin JH. Fluorometric and liquid chromatographic study of the binding of two coumarins to betacyclodextrin. Chirality. 1991;3:124–128.

29. Thuaud N, Sebille B, Deratani A, Lelievre G. Determination by high-performance liquid chromatography of the binding properties of charged .beta.-cyclodextrin derivatives with drugs. J Chromatogr. 1990;503:453–458.

30. Jones G, Vullev VI. Contribution of a pyrene fluorescence probe to the aggregation propensity of polypeptides. Org Lett. 2001;3: 2457–2460.

31. Jones G, Vullev VI. Ground- and excited-state aggregation properties of a pyrene derivative in aqueous media. J Phys Chem A. 2001;105.

32. Valente EJ, Lingafelter EC, Porter WR, Trager WF. Structure of warfarin in solution. J Med Chem. 1977;20:1489–1493.

33. Valente EJ, Trager WF. Anomalous chiroptical properties of warfarin and phenprocoumon. J Med Chem. 1978;21:141–143.

34. Karlsson B, Rosengren AM, Andersson PO, Nicholls IA. The spectrophysics of warfarin: implications for protein binding. J Phys Chem B. 2007;111:10520–10528. 35. Lide DR. CRC Handbook of Chemistry and Physics, 88 ed. Taylor and Francis; 2007. AQ4

36. Kasai-Morita S, Horie T, Awazu S. Influence of the N-B transition of human serum albumin on the structure of the warfarinbinding site. Biochim Biophys Acta. 1987;915:277–283.

37. The Dow Chemical Company, Viscosity of Aqueous Glycerine Solutions. http://www.dow.com/glycerine/resources/table18.html.

38. Dorsey NE. Properties of Ordinary Water Substances. Reinhold, New York; 1940.AQ5

39. Tu C-H, Lee SL, Peng JI-H. Excess volumes and viscosities of binary mixtures of aliphatic alcohols (C1-C4) with nitromethane. Chem Eng Data. 2001;46:151–155. 40. Saleh MA, Akhtar S, Begum S, Ahmed MS, Begum SK. Density and viscosity of 1-alkanols. Phys Chem Liq. 2004;42:615– 623.

41. Panadero S, Gomez-Hens A, Perez-Bendito D. Simultaneous determination of warfarin and bromadiolone by derivative synchronous fluorescence spectrometry. Talanta. 1993;40:225–230.

42. Eastman JW. Quantitative spectrofluorometry: the fluorescence quantum yield of quinine sulfate. Photochem Photobiol. 1967;6: 55–72.

43. Fletcher AN. Quinine sulfate as a fluorescence quantum yield standard. Photochem Photobiol. 1969;9:439–444.

44. Valeur B. Molecular Fluorescence: Principles and Applications. Wiley-VCH; 2002:387. 45. Lip GYH, Lim HS. Atrial fibrillation and stroke prevention. Lancet Neurol. 2007;6:981–993.

Chapter 3

Seeing warfarin in biological fluids: Facile quantification of the concentration of a potent anticoagulant in blood plasma

CHAPTER 3. Seeing warfarin in biological fluids: Facile quantification of the concentration of a potent anticoagulant in blood plasma

Abstract

Warfarin is an oral anticoagulant drug used in the treatment of various cardiovascular and cerebrovascular disorders. It is a drug with a narrow therapeutic index placing a strict requirement for careful monitoring of the patients taking it. In order to ensure that the effective physiological result is achieved and maintained, the dose must be adjusted accurately and frequently. Currently, estimation of the international normalized ratio (INR) of the prothrombin time (PT) is the most common method used for monitoring warfarin therapy. This estimation is actually a measure of the physiological result of a dose taken up to 72 hours prior. A rapid and clinically deployable methods for measuring warfarin in blood plasma in real-time are needed in combination with PT/INR to further predict and prevent lapses in patient compliance, such as changes in diet and interactions with other medications, that result in falling out of the warfarin therapeutic range. Here we describe a rapid extraction of warfarin from aqueous samples, including from blood plasma, and quantifying the extracts using fluorescence spectroscopy. Warfarin absorbs and emits in the UV spectral range, which presents a principle challenge for its detection and quantification in biological samples using inherently sensitive fluorescence methods. Warfarin is a phenolic acid with pKa between about 5 and 6. Thus, its spectral properties and its extraction propensity manifest strong pH dependence. We demonstrate that lowering the pH improves the extraction of warfarin from aqueous into organic media.

Conversely, an increase in the media basicity causes a considerable increase in its fluorescence quantum yield accompanied by bathochromic spectral shifts. Therefore, a facile adjustment of the acidity of samples and extracts makes a huge improvement in the ability to detect and quantify warfarin. Furthermore, the pH dependence of the spectral properties of warfarin provides a potential means for quantifying this drug in the presence of fluorescent contaminants. We believe that the protic transformations of warfarin open unexplored routes for its facile and rapid quantification with potential clinical importance.

3.1 Introduction

Racemic warfarin, a vitamin K antagonist, has been prescribed for more than 5 decades as an oral anticoagulant and rodenticide.[45] Warfarin prevents the clotting of blood through competitive inhibition of vitamin K epoxide reductase. [2] While its two enantiomers do not exhibit equivalent activity due to differences in drug/enzyme pharmacokinetics and rates of metabolism, they complement each other regarding initial activity and duration of the effects. The wide use of this orally administrated anticoagulant includes treatment and prevention of thromboembolic disorders (arterial and venous thromboemboli).[46] The physiological consequences of this therapeutic manifest in a decrease in the propensity for forming blood clots that results from lowered activity of important vitamin-K-dependent clotting factors.

Despite its therapeutic benefits, over and under-coagulation must be avoided due to potential life-threatening complications.[47]In fact, warfarin was discovered in 1939 from an

investigation of unexpected massive deaths of life stock in farms in Wisconsin.[48] Also, this natural product, a derivative of coumarin, is named after the Wisconsin Alumni Research Foundation (WARF) that funded the investigation.[49] Because of its potent physiological effects, warfarin was commercialized initially as a rat poison.[50]

The clinical potential of the drug was not fully realized until 1951, when a man purposely ingested a large amount of warfarin formulated as rat poison. The subsequent survival of this patient, reignited interest in warfarin as a potential therapeutic in humans. The first clinical study using warfarin followed shortly thereafter in [7]1955. [ref] Additionally, warfarin was given to President Dwight Eisenhower that same year following a myocardial infarction.

The mean(range) steady state, physiological plasma concentrations of warfarin in therapeutic and chronically anticoagulated patients is approximately 6.5(4.5-11.4)μM and 10.1(5.5–22)μM, respectively.[51] Depletion of warfarin from patients given a single oral dose, showed that up to 25% of the peak plasma concentration can be lost in 24 hours, highlighting the importance of patient compliance and dose monitoring.[51–56] This rapid depletion of plasma concentration highlights one of the biggest drawbacks of warfarin, its narrow therapeutic index (NTI). In addition to its small TI, the variability in dose response, interactions with other blood factors and therapeutics, changes in diet, and genetics, make careful monitoring and regulating of warfarin paramount for patients taking this drug.[57–61] The accepted way for warfarin and its physiological effect to be monitored is via the prothrombin time, PT/INR (PT/INR = $[PT_{patient}/PT_{conrol}]^{ISI}$).[46] This clot time (PT/INR) is calculated as the patient's PT divided by a control PT, raised to the power of the

international sensitivity index (ISI). The ISI is specific for each lot of thromboplastin reagent, and is provided by commercial vendors. The PT/INR test utilizes blood plasma, calcium and thromboplastin, which upon mixing, forms a fibrin clot.[46] Various commercial automated analyzers utilize physical characteristics of clot formation (changes in translucency, color and viscosity) to determine the time in seconds for the clot to form.[62] A normal INR for someone not on anticoagulation therapy is 0.8-1.2.[46,62]

For most all of patients under warfarin therapy, the warfarin dose that is targeted is the dose that gets the INR in the range between 2.0 and 3.0. This INR range was empirically determined[46] to balance the benefit of prevention of clot formation (with increasing warfarin dose), with the probability (incidence) of a major bleeding event occurring. Indeed, many factors affect the ability of warfarin to influence the INR in a dose-dependent manner including diet, e.g., eating vegetables with high vitamin K content that antagonizes the effect of warfarin on the INR. Numerous drug-drug interactions can also affect the physiology of warfarin. Such interaction can be direct, such as amiodarone (antiarrhythmic agent) and statins (lowers lipids; prescribed for cardiovascular disease),[63,64] and indirect, e.g., all antibiotics result in an increase of the INR at any warfarin dose. Other factors include genetics, age and concurrent cardiac, renal and hepatic disease.[64] Another major side effect of warfarin, which is not related to bleeding, is skin necrosis. While this conditions is exceptionally rare, it is extremely disfiguring and potentially life threatening. The mechanism by which this skin condition occurs is due to the fact that anticlotting factor protein C has a shorter half-life time than the proclotting factors affects by warfarin. Initiation of warfarin therapy results in a rapid depletion of protein C relative to the other

vitamin-K dependent factors during warfarin therapy, which results in microthrombi developing in the skin and soft tissue.[65]

Dabigatran etexilate (Pradaxa),[66] rivaroxaban (Xarelto)[67], and apixaban (Eliquis)[68] are new oral anticoagulants available as alternatives to warfarin in the US and Europe. Unlike warfarin, these new anticoagulants, Direct Oral Anticoagulants (DOACs), exhibit predictable dose responses and do not require routine coagulation monitoring, but their anticoagulation effect declines quickly when patient compliance is lacking. In addition, no standardized coagulation monitoring tests are currently recommended or recommended for these tests.[69] Protocols to address anticoagulant-related bleeding also differs between warfarin and the new classes of DOACs. Warfarin related bleeds can be mitigated/reversed by administration of intravenous vitamin K, however, reversal agents have only recently been introduced into the market (intravenous administration of monoclonal antibodies to bind excess drug) for a few of the new DOACs, complicating emergency treatment where life threating bleeds related new DOACs are involved.[70,71] Despite the promise of these other oral anticoagulants, warfarin remains the most prescribed blood thinner in the world, whose use contributes to the second most emergency room visits annually.

Concurrently, warfarin is a coumarin, i.e., a strongly fluorescent chromophore.[72] The inherent sensitivity of fluorescence spectroscopy and imaging makes them a preferred approach for biological, medical and biosensing applications.[73–76] Warfarin, however, absorbs and emits in the UV region of the spectrum (Figure 1),[32] making it immensely challenging for analysis of its content in blood samples, especially when the concentration ranges of clinical interest are in the micromolar and submicromolar ranges.[51–56] The

usefulness of fluorogenic agents absorbing and emitting in the visible spectral region would require molecular designs that offer high affinity and specificity for warfarin (i.e., with dissociation constants in the nanomolar range), along with a sharp spectral response upon binding of this coumarin derivative.

Indeed, the inherent background emission of blood samples renders fluorescence methods impossible for detection and quantification of warfarin in such biological fluids. Nevertheless, extraction of warfarin with common organic solvents and its chromatographic quantification presents an alternative.[77,78] High-pressure liquid chromatography (HPLC) required for such analysis, however, tends to be challenging for clinical settings.

Herein, we focus on the possibility of extracting warfarin from blood plasma samples. Optimization of the extraction procedure, minimizing the volume of samples and maximizing the possible concentrations in the organic extracts, are key parameters for viable fluorescence analyses. The strong dependence of the warfarin absorption and emission on the media acidity allows for addressing key challenges for quantification of this drug in the presence of contaminants exhibiting similar absorption and fluorescence.

3.2 Results and Discussion

3.2.1 Protic equilibria.

The acidity of its phenolic hydroxyl ($pK_a \approx 5.1 – 5.6$),[32] the propensity for tautomerization and its inherent chirality results in more than 40 different structures of warfarin.[79,34,80] In

aqueous media, under physiological pH, warfarin is deprotonated with the negative charge distributed over the oxygens bonded to the lactone coumarin ring. An increase in the media acidity yields the protonated forms of warfarin that predominately exist as cyclic hemiketals, i.e., closed-ring tautomers (Scheme 1). Nucleophilic attacks of the oxygens bonded to carbons 2 or 4 on the carbonyl carbon, 3', generates a second chiral center and a six-member ring with a pronounced stability. Non-polar media especially favors this tautomerization leading to the closed forms.[72,34]

This protic equilibrium and tautomerization greatly affects the spectral properties of warfarin.[80] We focus on the UV absorption and emission behavior of warfarin dissolved in 1-octanol under acidic and basic conditions. Under basic conditions the maximum of the warfarin fluorescence is at 395 nm with a Stokes' shift of 85 nm (Figure 1a). Acidifying the media quenches the fluorescence of warfarin and results in hypsochormism of its absorption and the emission, yielding fluorescence maximum at 355 nm and a Stokes' shift of 52 nm (Figure 1b). The fluorescence quantum yield of warfarin for media where the cyclic form is predominant is about 5-11 times smaller than the quantum yield of warfarin for solutions where the open-form isomers are abundantly present.[34]Therefore, basifying the samples, especially when non-polar organic solvents are used, is immensely important for fluorescence sensing of warfarin.

The concentration dependence of the fluorescence intensity of warfarin under basic conditions shows nonlinearity for $C_{warfarin} > 20$ μM, while the absorbance shows linearity through the investigated concentration range (Figure 2). This emission trend can be ascribed to the inner-filter effects accompanied by the inherent non-linear relationship

between fluorescence intensity and concentration. The latter can be expressed in terms of a power-law that converts absorbance (and its linear concentration dependence) to intensity of absorbed light:[81,82]

$$F(C) = \Delta F(1 - 10^{-aC}) \quad \text{(eq. 1)}$$

Where $F(C)$ is the emission intensity of warfarin, ΔF is the maximum possible increase in fluorescence, and α accounts for the molar extinction coefficient and the effective thickness of the sample.

Despite the non-linearity, the concentration-dependence curve for warfarin fluorescence under basic conditions (Figure 2c, inset) shows largest steepness for $C_{warfarin} \leq 20$ μM, i.e., the concentration range of greatest clinical importance.

3.2.2 Extraction of warfarin from aqueous solutions.

The acidity of the environment affects the warfarin charge, i.e., under basic conditions, the deprotonated open forms of warfarin are negatively charged and hence, with an increased water solubility. Therefore, we expect that acidic conditions improve the extraction efficiency of warfarin from aqueous into organic media. Indeed, as we determined using UV absorption spectroscopy, extracting from acidic samples results in 3-fold larger amount of warfarin that is transferred than from basified samples.

The concentration of warfarin extracted in the organic phase, [W_{oct}], is important for quantification of its concentration in the aqueous samples, C_0. Indeed, C_0 shows a linear relationship with [W_{oct}] that depends on the distribution coefficients, K_D, for warfarin under the conditions of the extraction; and on the volumes of the organic, V_{oct}, and the aqueous, V_{aq}, phases after the extraction. Namely:

$$K_D = \frac{[\mathrm{W_{octanol}}]}{[\mathrm{W_{aqueus}}]} \quad \text{(eq. 2a)}$$

$$\gamma V_{aq} C_0 = V_{aq}[W_{aq}] + V_{oct}[W_{oct}] \quad \text{(eq. 2b)}$$

$$C_0 = (K_D^{-1} + 1)\frac{V_{oct}}{\gamma V_{aq}}[W_{oct}] \quad \text{(eq. 2c)}$$

Where [$W_{aqueous}$] is the concentration of warfarin in the water phase after the extraction, and □ accounts for the procedural dilutions of the samples prior to the extraction. In the presence of bovine serum albumin (BSA, 100 mg/ml) in the aqueous samples, the obtained values for K_D, ranging from 1.5 to 1.8 (Table 1).

Keeping the volume of the organic phase much smaller than the volume of the aqueous one allows for improving the sensitivity and for lowering the detection limits. That

is, a decrease in the slope in eq. 2c ensures that small changes in C_0 would result in larger changes in [W_{oct}]. Indeed, the practical decrease this volume ratio, V_{oct}/V_{aq}, is limited by how large the aqueous warfarin samples and how small the octanol extracts can practically be.

3.2.3 Extraction of warfarin from samples of blood plasma

Therefore, for the test in this study, we carry out the extractions under acidic conditions, employing small V_{oct}/V_{aq} ratios, and the spectroscopic measurements after basifying the organic samples. Namely, we add known amounts of warfarin to 1.25 mL sample. Addition of 0.5 ml of 10 % trichloroacetic acid (TCA) allows for acidifying the media and denaturing the proteins that may be present in the samples. If proteins are present, we observed formation of precipitate, which we separate via centrifugation. We collect 1.25 ml of the clear supernatant, and add 0.075 ml NaOH (to buffer the solution to pH 2), 0.25 ml of a dispersing agent, methanol and 0.25 ml of 1-octanol for extraction of the warfarin. After vigorous shaking, we collect the organic phase that we examine using UV absorption and fluorescence spectroscopy. Because of the bathochromic spectral shifts and the increase in the fluorescence quantum yield of warfarin when increasing the pH, we add an organic base, 1-hexylamine, to eliminate the cyclic forms prior to the spectroscopy analysis. Methanol transfers to the aqueous phase and plays a role of dispersant. The methanol is necessary to allow for proper emulsification and contact between the two phases. (The dispersant must be miscible in both the organic and aqueous phases to allow

for proper emulsification). Without methanol, the octanol beads up quickly and does not form small droplets and emulsify. Emulsification provides the needed large contact area between the octanol and the aqueous sample. Our attempts to carry out extractions without methanol leads to negligible amounts of warfarin transferred to the organic phase.

Even at such disproportionally small ratios between the volumes of the octanol extract and the aqueous sample, the extraction efficiency, EE, is about 20% for micromolar initial concentrations of warfarin in the aqueous samples, C_0 (Figure 4, Table 2).

$$\mathrm{EE} = \frac{n_{\mathrm{oct}}}{n_{\mathrm{aq}}{}^{(0)}} \qquad \text{(eq. 3)}$$

Where n_{oct} is the amount of moles of warfarin extracted in the organic phase and $n_{\mathrm{aq}}{}^{(0)}$ is the moles of warfarin in the aqueous phase prior to the extraction. Consistent EE across a wide range of sample concentrations shows that the EE has negligible dependence on analyte concentration, C_0 (Figure 4).

Using UV absorption spectroscopy is relatively straightforward for determining the warfarin concentrations in the octanol extracts because of the linearity provided by the Bouguer-Lambert-Beer law. The inherent sensitivity of fluorescence makes it a more attractive approach for estimating the warfarin concentrations in the extracts. Because of the fluorescence non-linear concentration dependence, we employ calibration curves of intensity vs. known warfarin concentration for octanol in the presence of hexylamine, for quantifying warfarin from its emission spectra (Figure 2c, inset). The concentrations of warfarin extracted from BSA solutions determined from fluorescence intensities match

well with the concentrations of the same samples obtained using absorption spectroscopy (Table 2).

To evaluate the accuracy and applicability of this approach to biological samples, we perform extraction and quantitative analysis of warfarin dissolved in blood plasma, using the same sample volumes as previous described. Fluorescence analysis of extracts from blood-plasma samples yields values for [W_{oct}]. The thus obtained warfarin concentrations excellently match with the concentrations obtained for extraction of warfarin from BSA samples (Table 2).

3.2.4 Quantification of warfarin in the presence of fluorescent contaminants.

Despite the promising potential of the described spectroscopic quantification of warfarin, co-extraction of endogenous and exogenous fluorescent contaminants presents a challenging limitation. The pH dependence of the absorbance and fluorescence properties of warfarin offers a means for addressing this challenge. Under acidic conditions the fluorescence quantum yield of warfarin is considerably smaller, than under basic conditions (Figure 1).[83]Therefore, recorded emission spectra of the acidified octanol extracts prior to the addition of the organic base can serve as a baseline for the analysis. That is, instead of using only fluorescence intensities of the basified octanol extracts for quantification of warfarin, we can use the difference in fluorescence intensities between the basic and acidic octanol solutions.

To test the validity of this approach, we used 7-methoxycoumarin (7MC) as a model of a fluorescent contaminant. The absorbance and fluorescence spectra of 7MC have excellent overlap with the absorbance and fluorescence of warfarin, making it immensely challenging to discern the spectra of the 2 fluorophores. Furthermore, the fluorescence quantum yield of 7MC is 0.16.[83] Therefore, even minute amounts of this contaminant can have pronounced contribution to the measured fluorescence spectra. The absorbance and fluorescence spectra of 7MC in octanol show relatively small dependence on acidity of the media (Figure 8).

To test the influence of this contaminant on the fluorescence quantification of warfarin, we add 5 μM of 7MC to different octanol extracts of warfarin from blood plasma. We observe a significant difference between the fluorescence intensities of warfarin/7MC samples measured under acidic conditions (Figure 8). We ascribe this difference predominantly to the presence of warfarin and use it for its quantification in the warfarin/7MC samples. Indeed, for this analysis, we prepare calibration curves based on the differential fluorescence of warfarin samples with known concentrations. For the same C_0, the thus obtained warfarin concentrations, $[W_{oct}]$, for the contaminated samples are similar to the concentrations we observed for extracts without a contaminant (Figure 8c). The difference in fluorescence for basic and acidic conditions, therefore, is representative of the amount of warfarin in the samples.

The excellent match between the concentration value obtained for warfarin in the presence and absence of a contaminant shows the unexplored potential of the utility of differential-emission analysis for quantification of this anticoagulant medication.

3.4 Conclusions.

Microextraction, coupled with absorbance and fluorescence spectroscopic analysis, provides a means for a relatively simple method for quantification of warfarin in blood samples. We utilize the inherent pH-dependent tautomerization of warfarin for optimization of its extraction efficiency and spectroscopic quantification. This pH dependence proved especially important for utilizing differential emission for eliminating the adverse effect from fluorescent contaminants. This method offers working range across the physiologically relevant concentrations, while utilizing relatively small volumes of biological sample.

3.5 Experimental

Materials

Racemic warfarin (4-hydroxy-3(3-oxo-1-phenylbutyl) coumarin, min 98%) was obtained from Sigma-Aldrich (St. Louis, MO). Water used was Millipore grade (Millipore, Bedford, MA). Organic solvents 1-Octanol and Methanol were of (spectroscopic grade), 1-Hexylamine and bovine serum albumin, fraction V, were obtained from Sigma-Aldrich (St. Louis, MO). Sodium hydroxide and trichloroacetic acid were obtained from Fisher-Scientific (Hampton, NH). Fetal bovine blood serum was obtained from Thermo-Fisher-Life Technologies-Gibco (Pleasanton, CA).

Methods

Extraction assays. Stock solution of 10 mM warfarin in methanol was prepared. Three aqueous samples were used: (1) 100 mM phosphate-buffered saline (PBS); (2) 100 g/ml bovine serum albumin (BSA) and 100mM PBS; and (3) blood plasma. Different amounts of warfarin stock solution, 10 mM were added to 1.25 ml aqueous samples to bring the warfarin to different concentrations, C_0. Each 1.25-ml aqueous sample was diluted with 10 % water solution of TCA to bring it to final volume of 1.75 ml. The mixture was vortexed for 20 s, and incubated at room temperature for 5 min. If protein was present, a precipitate formed. The sample was centrifuged for 2 min at 12,000 rpm and 1.25 mL of the clear supernatant was collected and placed into a 2-ml centrifuge tube. 0.075 ml of 1N NaOH was added to the collected supernatant to adjust its pH to about 2. An 1-octanol/methanol solution (1/1 v/v, 0.5 ml) was mixed with the aqueous supernatant, vortexed for 1 min, and centrifuged for 2 minutes at 12,000 rpm. The final volume of the organic phase, Voct, was 0.25 ml, and of the aqueous phase – 1.575 ml. 0.12 ml of the organic phase were collected and basified with 10 □l 1-hexylamine.

For extraction under basic conditions, the same procedure was followed but Milli Q water was added instead of a TCA solution. For spectral measurement of acidic samples, the 1-hexylamine was not added.

UV absorption spectroscopy. UV/Visible absorption spectra measurements were scanned at room temperature, between 260 and 500 nm on a JASCO Varian Cary V-670 spectrophotometer (Tokyo, Japan). Quartz cuvettes (1.0 cm, 0.1 mL) were used in all spectroscopic measurements, obtained from Starna Cells Inc. (Atascadero, CA).

Fluorescence spectroscopy. Fluorescence emission spectra measurements were scanned at room temperature, between 325 and 550 nm with a Jobin-Yvon HORIBA Fluorolog-3-22 fluorimeter, slit width, 4.0 nm (Edison, New Jersey).

3.6 Schemes

Scheme 3-1. Dynamic Equilibrium of Warfarin Structure In Solution

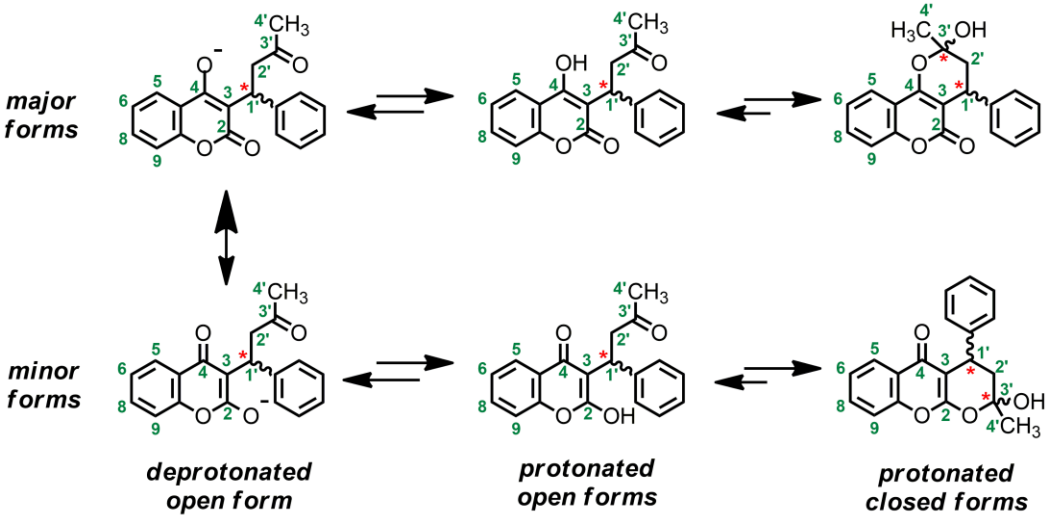

3.7 Figures

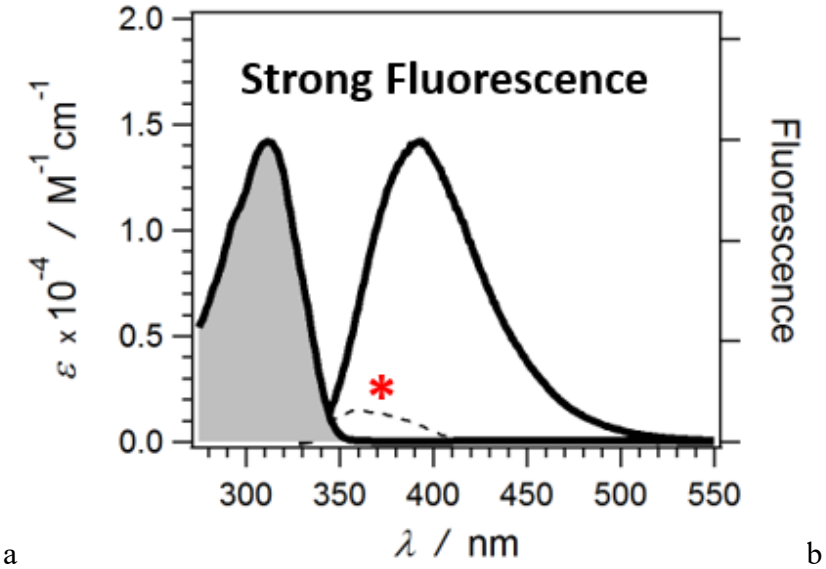

a b

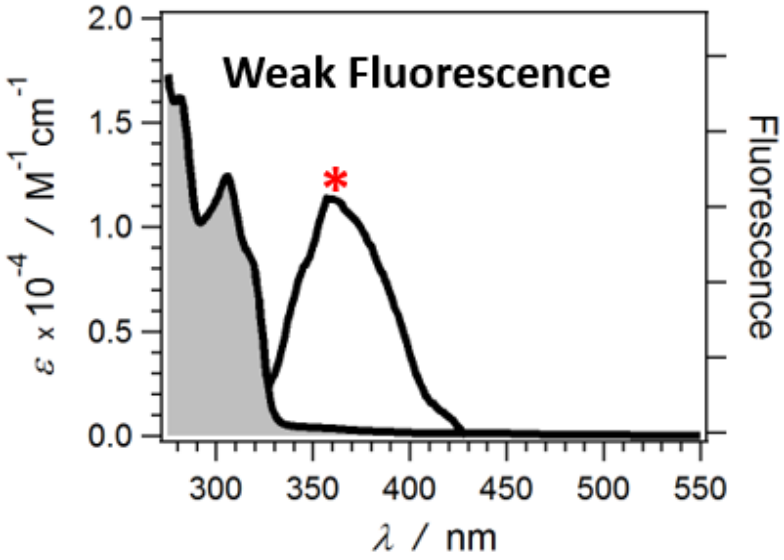

Figure 3-1. Dependence of absorbance and fluorescence of warfarin for acidic and basic conditions (λ_{ex} = 310 nm). (a) Absorption and emission spectra of 50 µM warfarin dissolved in 1-octanol in the presence of 8% (v/v) hexylamine and 25mM deproteinating agent trichloroacetic acid. ε_{W50} = 10,607 L mol^{-1}cm^{-1} (b) Absorption and emission spectra of 50 µM warfarin dissolved in 1-octanol in the presence of 25 mM deproteinating agent trichloroacetic acid. For comparison, the emission spectrum for acidic media is included in (a) and designated with *.

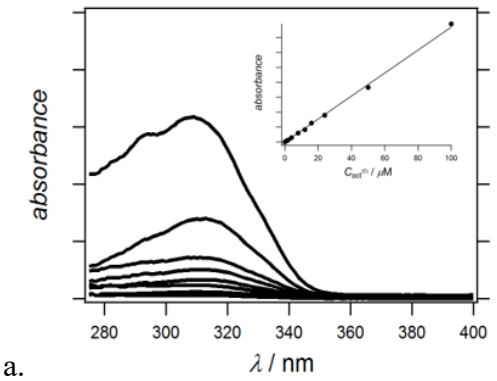

a.

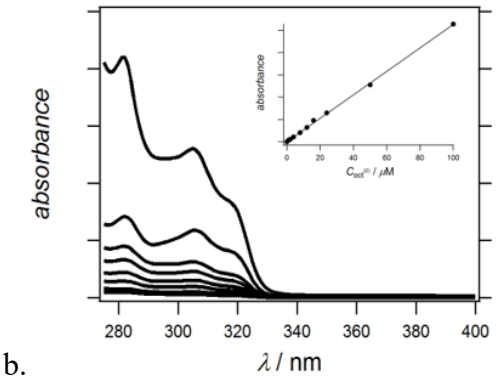

b.

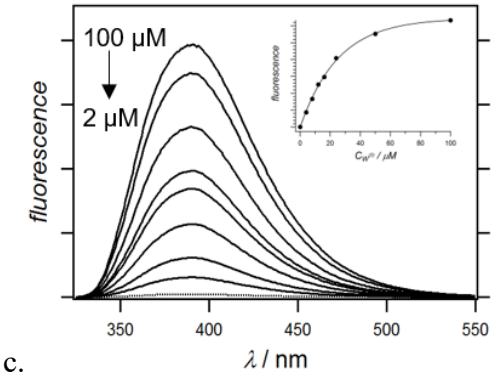

c.

Figure 3-2. Concentration dependence of absorbance and fluorescence of warfarin (2 – 100 □M) for 1-octanol. (a) Absorption spectra in the presence of 8 % v/v. (b) Absorption spectra in the presence of 25 mM trichloroacetic acid. Insets of (a) and (b): concentration dependence of the absorbance at 310 nm. (c) Fluorescence spectra in the presence of 8 % v/v (λ_{ex} = 310 nm). Inset of (c): Dependence of integrated emission intensity on warfarin concentration with a non-linear fit is based on eq. 1.

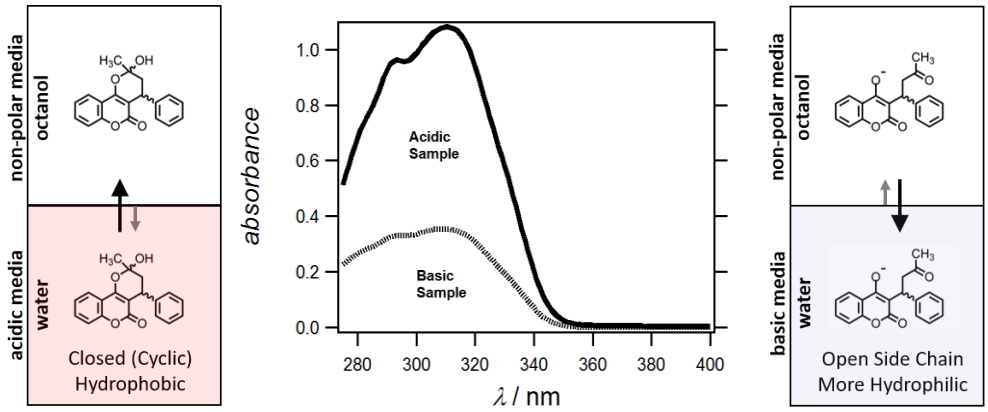

Figure 3-3. Acidic vs. basic conditions for extraction of warfarin into 1-octanol. Absorption spectra of warfarin extracted into 1-octanol from acidic (solid) and basic (dashed) aqueous solutions of 25 µM warfarin. (10 µl 1-hexylamine were added to 0.120 ml of the octanol extract prior to recording the spectra.)

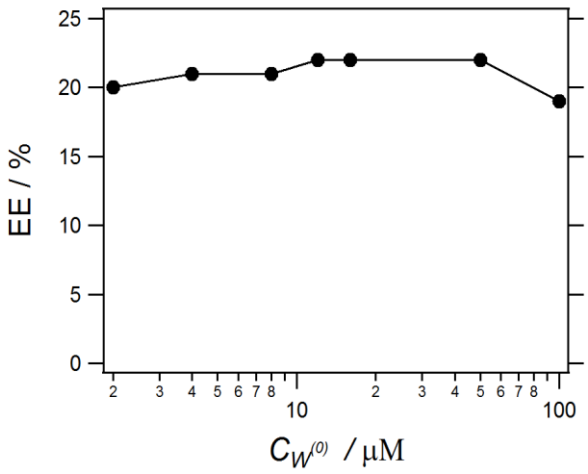

Figure 3-4. Concentration dependence of the extraction efficiency, EE, of warfarin from aqueous solutions of BSA in 1-octanol.

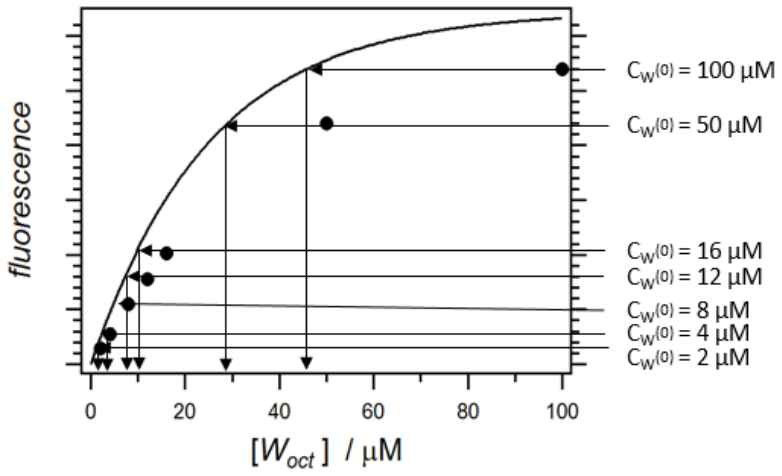

Figure 3-5. Interpolative estimation of warfarin concentration from integrated fluorescence of octanol extracts. The calibration curve is obtained from the fluorescence spectra of octanol solutions of warfarin with known concentrations. The octanol extracts are from aqueous samples with different concentration of warfarin, C_0, containing 100 mg/mL BSA.

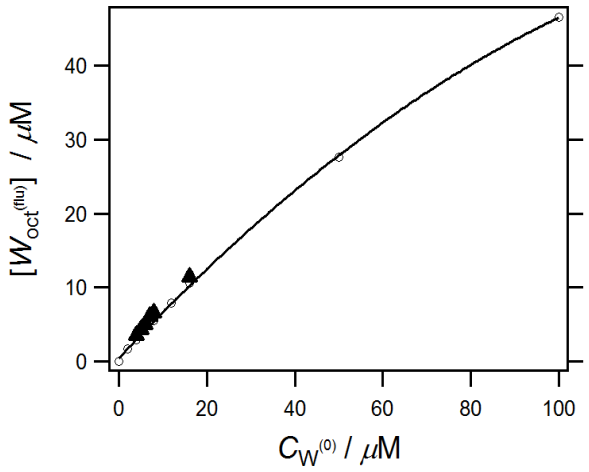

Figure 3-6. Concentration dependence of fluorescence of warfarin for 1-octanol (λ_{ex} = 310 nm). Dependence of integrated emission intensity spectra for different concentrations of warfarin extracted from aqueous solution (2 – 100 µM) in1-octanol (open circle). Concentration dependence of warfarin extracted from blood plasma (solid triangle). The non-linear fit is based on eq. 1.

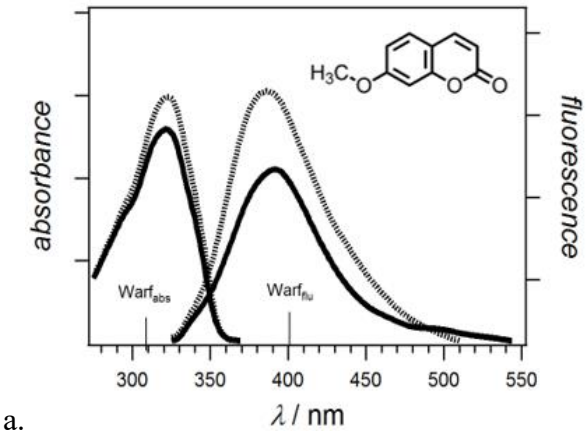

a.

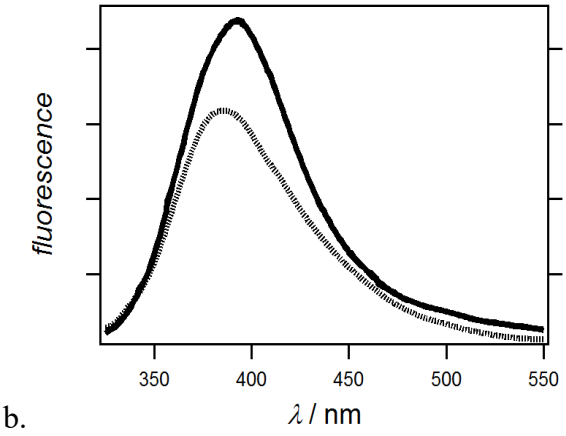

b.

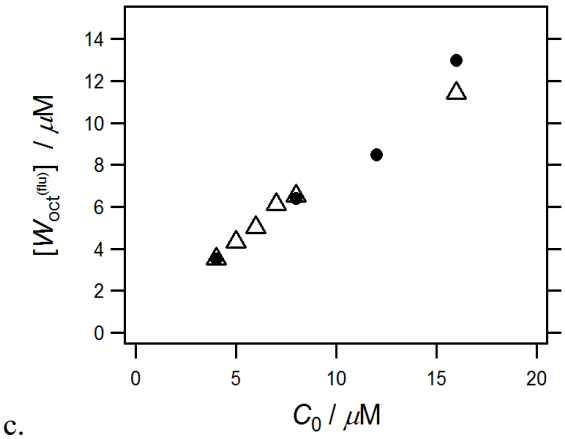

c.

Figure 3-8. Dependence of absorbance and fluorescence of 7-methoxycoumarin (7MC) for acidic and basic conditions (λ_{ex} = 310 nm). (a) Absorption and fluorescence spectra of 5 µM 7MC dissolved in 1-octanol. (b) Emission spectra of acidic and basic octanol extracted from blood plasma (4 µM warfarin + 5 µM 7MC). (c) Concentration comparison of warfarin extracted from plasma with and without contaminants.

3.8 Tables

Table 3-1. Extraction of warfarin from acidified aqueous in 1-octanol.[a]

C_0 / μM [b]	[W_{aq}] / μM [c]	[W_{oct}] / μM [c]	K_D	$n_{aq}^{(0)}$ / nmol	n_{oct} / nmol	EE / %
2	0.91	1.4	1.6	1.4	0.36	20%
4	1.8	3.0	1.7	2.8	0.74	21%
8	3.6	6.1	1.7	5.6	1.5	21%
12	5.3	9.5	1.8	8.3	2.4	22%
16	7.1	12	1.8	11	3.1	22%
50	22	40	1.8	35	9.9	22%
100	46	69	1.5	72	17	19%

[a] 1.25 ml acidified aqueous sample, 0.25 ml 1-octanol, and 0.25 ml methanol. [b] Initial warfarin concentration in the aqueous sample prior to acidification and dilution. [c] Concentrations obtained from absorption measurements.

Table 3-2. Interpolated concentration from bovine serum albumin and blood plasma

C_0 / μM BSA	[$C_{W(flu)}$] / µM $Fi_{Interpol}$ / Eq. 1¥	C_0 / μM Blood Plasma	[W_{oct}] / μM $Fi_{Interpol}$ / Eq. 1¥
2	1.7	4.0	3.5
4	2.9	5.0	4.3
8	5.5	6.0	5.0
12	7.9	7.0	6.1
16	10.6	8.0	6.5
50	27.6	16.0	11.4
100	46.6		

¥; Dose values were interpolated from basic 1-octanol curve using equation (1)

Table 3-3. Interference of 7-methoxycoumarin on dose recovery

C_0 / μM	[W_{oct}] / μM
4.0	3.5
8.0	6.4
12.0	8.5
16.0	13.0

3.9 References

(1) Otagiri, M.; Fokkens, J. G.; Hardee, G. E.; Perrin, J. H. Pharm. Acta Helv. 1978, 53 (8), 241–247.

(2) Bristol-Meyers Squibb Company. 2007.

(3) Park, B. K. Biochem. Pharmacol. 1988, 37 (1), 19–27.

(4) Büller, H. R.; Agnelli, G.; Hull, R. D.; Hyers, T. M.; Prins, M. H.; Raskob, G. E. Chest 2004, 126 (3 Suppl), 401S – 428S.

(5) Albers, G. W.; Amarenco, P.; Easton, J. D.; Sacco, R. L.; Teal, P.; American College of Chest Physicians. Chest 2008, 133 (6 Suppl), 630S – 669S.

(6) Loftsson, T.; Brewster, M. E. J. Pharm. Sci. 1996, 85 (10), 1017–1025.

(7) Singer, D. E.; Albers, G. W.; Dalen, J. E.; Fang, M. C.; Go, A. S.; Halperin, J. L.; Lip, G. Y. H.; Manning, W. J.; American College of Chest Physicians. Chest 2008, 133 (6 Suppl), 546S – 592S.

(8) J. Am. Geriatr. Soc. 2000, 48 (2), 224–227.

(9) Herman, D.; Locatelli, I.; Grabnar, I.; Peternel, P.; Stegnar, M.; Mrhar, A.; Breskvar, K.; Dolzan, V. Pharmacogenomics J. 2005, 5 (3), 193–202.

(10) Takahashi, H.; Wilkinson, G. R.; Nutescu, E. A.; Morita, T.; Ritchie, M. D.; Scordo, M. G.; Pengo, V.; Barban, M.; Padrini, R.; Ieiri, I.; Otsubo, K.; Kashima, T.; Kimura, S.; Kijima, S.; Echizen, H. Pharmacogenet. Genomics 2006, 16 (2), 101–110.

(11) Schulman, S.; Beyth, R. J.; Kearon, C.; Levine, M. N.; American College of Chest Physicians. Chest 2008, 133 (6 Suppl), 257S – 298S.

(12) FDA. FDA News FDA Approves Updated Warfarin (Coumadin) Prescribing Information: New Genetic Information May Help Providers Improve Initial Dosing Estimates of the Anticoagulant for Individual Patients.; 2007.

(13) Badía, R.; Díaz-García, M. E. J. Agric. Food Chem. 1999, 47 (10), 4256–4260.

(14) Márquez, J. C.; Hernández, M.; García Sánchez, F. The Analyst 1990, 115 (7), 1003–1005.

(15) Tang, L. X.; Rowell, F. J. Anal. Lett. 1998, 31 (5), 891–901.

(16) Al-Hassan, K. A.; Meetani, M. A.; Said, Z. F. M. J. Fluoresc. 1998, 8 (1), 93–100.

(17) Chen, J.; Ohnmacht, C. M.; Hage, D. S. J. Chromatogr. A 2004, 1033 (1), 115–126.

(18) Chen, W.; Chang, C.-E.; Gilson, M. K. Biophys. J. 2004, 87 (5), 3035–3049.

(19) Dondon, R.; Fery-Forgues, S. J. Phys. Chem. B 2001, 105 (43), 10715–10722.

(20) Hoshino, M.; Imamura, M.; Ikehara, K.; Hama, Y. J. Phys. Chem. 1981, 85 (13), 1820–1823.

(21) Lin, S. Y.; Yang, J. C. Pharm. Weekbl. Sci. 1986, 8 (4), 223–228.

(22) Otagiri, M.; Uekama, K.; Ikeda, K. Chem. Pharm. Bull. (Tokyo) 1975, 23 (1), 188–195.

(23) Sato, Y.; Suzuki, Y. Chem. Pharm. Bull. (Tokyo) 1985, 33 (10), 4606–4609.

(24) Wang, E.-J.; Lian, Z.-X.; Cai, J. Carbohydr. Res. 2007, 342 (5), 767–771.

(25) Zingone, G.; Rubessa, F. Int. J. Pharm. 2005, 291 (1-2), 3–10.

(26) Ishiwata, S.; Kamiya, M. Chemosphere 1997, 34 (4), 783–789.

(27) Karadaĝ, O.; Gök, E.; Serdar Ates, I.; Kiran, ö.; Bozkurt, A. J. Incl. Phenom. Mol. Recognit. Chem. 1994, 20 (1), 23–32.

(28) Karnik, N. A.; Prankerd, R. J.; Perrin, J. H. Chirality 1991, 3 (2), 124–128.

(29) Thuaud, N.; Sebille, B.; Deratani, A.; Lelievre, G. J. Chromatogr. A 1990, 503, 453–458.

(30) Jones, G.; Vullev, V. I. Org. Lett. 2001, 3 (16), 2457–2460.

(31) Jones, G.; Vullev, V. I. J. Phys. Chem. A 2001, 105 (26), 6402–6406.

(32) Valente, E. J.; Lingafelter, E. C.; Porter, W. R.; Trager, W. F. J. Med. Chem. 1977, 20 (11), 1489–1493.

(33) Valente, E. J.; Trager, W. F. J. Med. Chem. 1978, 21 (1), 141–143.

(34) Karlsson, B. C. G.; Rosengren, A. M.; Andersson, P. O.; Nicholls, I. A. J. Phys. Chem. B 2007, 111 (35), 10520–10528.

(35) Kasai-Morita, S.; Horie, T.; Awazu, S. Biochim. Biophys. Acta 1987, 915 (2), 277–283.

(36) Lide, DR. CRC Handbook of Chemistry and Physics, 88th ed.

(37) The Dow Chemical Company. Viscosity of Aqueous Glycerine Solutions.; 1999.

(38) Dorsey NE. Properties of Ordinary Water Substances; 81; New York, Reinhold, 1940.

(39) Tu, C.-H.; Lee, S.-L.; Peng, I.-H. J. Chem. Eng. Data 2001, 46 (1), 151–155.

(40) Saleh, M. A.; Akhtar, S.; Begum, S.; Ahmed, M. S.; Begum, S. K. Phys. Chem. Liq. 2004, 42 (6), 615–623.

(41) Panadero, S.; Gómez-Hens, A.; Pérez-Bendito, D. Talanta 1993, 40 (2), 225–230.

(42) Eastman, J. W. Photochem. Photobiol. 1967, 6 (1), 55–72.

(43) Fletcher, A. N. Photochem. Photobiol. 1969, 9 (5), 439–444.

(44) Valeur, B. Molecular fluorescence: principles and applications; Wiley-VCH: Weinheim ; New York, 2002.

(45) Wardrop, D.; Keeling, D. Br. J. Haematol. 2008, 141 (6), 757–763.

(46) Guyatt, G. H.; Norris, S. L.; Schulman, S.; Hirsh, J.; Eckman, M. H.; Akl, E. A.; Crowther, M.; Vandvik, P. O.; Eikelboom, J. W.; McDonagh, M. S.; Lewis, S. Z.; Gutterman, D. D.; Cook, D. J.; Schünemann, H. J. Chest 2012, 141 (2), 53S – 70S.

(47) Hamby, L.; Weeks, W. B.; Malikowski, C. Eff. Clin. Pract. ECP 2000, 3 (4), 179–184.

(48) Pirmohamed, M. Br. J. Clin. Pharmacol. 2006, 62 (5), 509–511.

(49) Francis, C. W. Hematology 2008, 2008 (1), 251–251.

(50) Nelson, A. T.; Hartzell, J. D.; More, K.; Durning, S. J. MedGenMed Medscape Gen. Med. 2006, 8 (4), 41.

(51) O'Reilly, R. A.; Aggeler, P. M. Circulation 1968, 38 (1), 169–177.

(52) Breckenridge, A.; Orme, M. Clin. Pharmacol. Ther. 1973, 14 (6), 955–961.

(53) O'Reilly, R. A.; Levy, G. J. Pharm. Sci. 1970, 59 (9), 1258–1261.

(54) Lilja, J. J.; Backman, J. T.; Neuvonen, P. J. Br. J. Clin. Pharmacol. 2005, 59 (4), 433–439.

(55) Lilja, J. J.; Backman, J. T.; Neuvonen, P. J. Clin. Pharmacol. Ther. 2007, 81 (6), 833–839.

(56) Midha, K. K.; McGilveray, I. J.; Cooper, J. K. J. Pharm. Sci. 1974, 63 (11), 1725–1729.

(57) Krothapalli Md, S.; Bhave Md Fhrs, P. D. J. Atr. Fibrillation 2016, 9 (2), 1451.

(58) Víquez-Jaikel, A.; Victoria Hall-Ramírez, null; Ramos-Esquivel, A. Int. J. Clin. Pharm. 2016.

(59) P Dobesh Pharm D, P.; Fanikos Mba R Ph, J. J. Atr. Fibrillation 2016, 9 (2), 1481.

(60) Hellyer, J. A.; Azarbal, F.; Than, C. T.; Fan, J.; Schmitt, S. K.; Yang, F.; Frayne, S. M.; Phibbs, C. S.; Yong, C.; Heidenreich, P. A.; Turakhia, M. P. Am. J. Cardiol. 2016.

(61) Arnao, V.; Riolo, M.; Tuttolomondo, A.; Pinto, A.; Fierro, B.; Aridon, P. Expert Rev. Neurother. 2016.

(62) Gosselin, R.; Owings, J. T.; White, R. H.; Hutchinson, R.; Branch, J.; Mahackian, K.; Johnston, M.; Larkin, E. C. Thromb. Haemost. 2000, 83 (5), 698–703.

(63) Juurlink, D. N. Can. Med. Assoc. J. 2007, 177 (4), 369–371.

(64) Jorgensen, A. L.; Al-Zubiedi, S.; Zhang, J. E.; Keniry, A.; Hanson, A.; Hughes, D. A.; Eker, D. van; Stevens, L.; Hawkins, K.; Toh, C. H.; Kamali, F.; Daly, A. K.; Fitzmaurice, D.; Coffey, A.; Williamson, P. R.; Park, B. K.; Deloukas, P.; Pirmohamed, M. Pharmacogenet. Genomics 2009, 19 (10), 800–812.

(65) Sahu, K. K.; Varma, S. C. Indian J. Med. Res. 2016, 143 (4), 528–529.

(66) Gao, X.; Yang, Y. M.; Zhu, J.; Dai, Y.; Tan, H. Q.; RE-LY Chinese Investigators. Zhonghua Xin Xue Guan Bing Za Zhi 2016, 44 (11), 929–934.

(67) Cohen, H.; Hunt, B. J.; Efthymiou, M.; Arachchillage, D. R. J.; Mackie, I. J.; Clawson, S.; Sylvestre, Y.; Machin, S. J.; Bertolaccini, M. L.; Ruiz-Castellano, M.; Muirhead, N.; Doré, C. J.; Khamashta, M.; Isenberg, D. A.; RAPS trial investigators. Lancet Haematol. 2016, 3 (9), e426–e436.

(68) Granger, C. B.; Alexander, J. H.; McMurray, J. J. V.; Lopes, R. D.; Hylek, E. M.; Hanna, M.; Al-Khalidi, H. R.; Ansell, J.; Atar, D.; Avezum, A.; Bahit, M. C.; Diaz, R.; Easton, J. D.; Ezekowitz, J. A.; Flaker, G.; Garcia, D.; Geraldes, M.; Gersh, B. J.; Golitsyn, S.; Goto, S.; Hermosillo, A. G.; Hohnloser, S. H.; Horowitz, J.; Mohan, P.; Jansky, P.; Lewis, B. S.; Lopez-Sendon, J. L.; Pais, P.; Parkhomenko, A.; Verheugt, F. W. A.; Zhu, J.; Wallentin, L.; ARISTOTLE Committees and Investigators. N. Engl. J. Med. 2011, 365 (11), 981–992.

(69) Wassef, A.; Butcher, K. Int. J. Stroke Off. J. Int. Stroke Soc. 2016, 11 (7), 759–767.

(70) Pinto, I.; Giri, A.; Arshad, U.; Gajra, A. Curr. Drug Saf. 2015, 10 (3), 208–216.

(71) Staerk, L.; Fosbøl, E. L.; Lip, G. Y. H.; Lamberts, M.; Bonde, A. N.; Torp-Pedersen, C.; Ozenne, B.; Gerds, T. A.; Gislason, G. H.; Olesen, J. B. Eur. Heart J. 2016.

(72) Vasquez, J. M.; Vu, A.; Schultz, J. S.; Vullev, V. I. Biotechnol. Prog. 2009, 25 (4), 906–914.

(73) Mac, J. T.; Nuñez, V.; Burns, J. M.; Guerrero, Y. A.; Vullev, V. I.; Anvari, B. Biomed. Opt. Express 2016, 7 (4), 1311.

(74) Gorham, R. D.; Nuñez, V.; Lin, J.-H.; Rooijakkers, S. H. M.; Vullev, V. I.; Morikis, D. J. Med. Chem. 2015, 58 (24), 9535–9545.

(75) Anvari; Lytle; Walker; Gupta; Vullev; Anvari. Int. J. Nanomedicine 2013, 1609.

(76) Thomas, M. S.; Nuñez, V.; Upadhyayula, S.; Zielins, E. R.; Bao, D.; Vasquez, J. M.; Bahmani, B.; Vullev, V. I. Langmuir 2010, 26 (12), 9756–9765.

(77) Qayyum, A.; Najmi, M. H.; Khan, A. M.; Abbas, M.; Naveed, A. K.; Jameel, A. Pak. J. Pharm. Sci. 2015, 28 (4), 1315–1321.

(78) Shen, Y.; Xiang, J.; Liang, M.; Yu, Q.; Nan, F.; Qin, Y. Sichuan Da Xue Xue Bao Yi Xue Ban 2016, 47 (1), 106–110.

(79) Karlsson, B. C. G.; Olsson, G. D.; Friedman, R.; Rosengren, A. M.; Henschel, H.; Nicholls, I. A. J. Phys. Chem. B 2013, 117 (8), 2384–2395.

(80) Guasch, L.; Peach, M. L.; Nicklaus, M. C. J. Org. Chem. 2015, 80 (20), 9900–9909.

(81) Xia, B.; Upadhyayula, S.; Nuñez, V.; Landsman, P.; Lam, S.; Malik, H.; Gupta, S.; Sarshar, M.; Hu, J.; Anvari, B.; Jones, G.; Vullev, V. I. J. Clin. Microbiol. 2011, 49 (8), 2966–2975.

(82) Wan, J.; Thomas, M. S.; Guthrie, S.; Vullev, V. I. Ann. Biomed. Eng. 2009, 37 (6), 1190–1205.

(83) Wenska, G.; Paszyc, S. Can. J. Chem. 1988, 66 (3), 513–516.